DYNAMIC MODELING OF THE PRELIMINARY TREATMENT WORKS AT THE 69TH STREET WASTEWATER FACILITY HOUSTON, TEXAS

A Project
Presented to
the Faculty of the Graduate Program
in Civil Engineering
University of Houston

In Partial Fulfillment
of the Requirements for the Degree
Master of Science in Civil Engineering

by
James E. Vanderwater
December, 1996

DYNAMIC MODELING
OF THE PRELIMINARY TREATMENT WORKS
AT THE 69TH STREET WASTEWATER FACILITY
HOUSTON, TEXAS

James E. Vanderwater

Research Advisor
Dr. Theodore G. Cleveland, Associate Professor
Civil and Environmental Engineering

Dr. K. H. Wang, Associate Professor
Civil and Environmental Engineering

Dr. Dennis A. Clifford, Professor and Chairman
Department of Civil and Environmental Engineering

December 13, 1996

TABLE OF CONTENTS

List of Tables

List of Figures

List of Appendices

1.0 SUMMARY

Two (2) numerical models are presented that simulate the influent channel of City of Houston's 69th Street Wastewater Treatment Plant. The models evaluate the impact of the sudden starting of one and two pumps. These pumps generate a shallow bore resulting in the sudden acceleration of the wastewater throughout the preliminary treatment works. The model demonstrates that the acceleration front reaches the aerated grit chambers with little dissipation. This disturbance may contribute to the flushing of inorganic solids.

The solution of two explicit numerical models are presented. The models are programmed into an Excel Spreadsheet for calculation. First the Method of Characteristics solves the governing equations for velocity and celerity. The model converts these values to flow rate and water surface elevation. Then the Lax-Wendroff solution technique for solving the Saint Venant Equation calculates the velocity and the water depth. Both models use a known upstream boundary and a sharp crested weir downstream boundary. The modeling duration is typically about sixty (60) seconds. The wave travels the 180-foot length of the channel within the first fourteen (14) seconds. The models produce some overshoot of the peak value. The length of the downstream weir is adjusted to minimize the overshoot. The Saint Venant Model has a more pronounced overshoot. But the Method of Characteristics produces more numerical dispersion when the Courant number is less than one.

The model uses an initial condition of steady state flow at 18.75 cubic feet per second (cfs). This is one fourth of the plants average daily flow. Since there are four influent channels, the models represent the system with one channel carrying one fourth of the flow. Then the channel's flow rate is suddenly increased to 47.7 cfs at time greater than zero. After resetting the model to the initial conditions, the flow rate is suddenly increased to 76.65 cfs. Also, a gradual increase and decrease in flow rate is evaluated.

The Method of Characteristics model is very useful when a constant cross section represents the system and an appropriate time step is chosen. The Saint Venant solution could be expanded to represent the geometry of the channel more closely. The choice of the downstream boundary presented problems. Because the weir system minimizes changes in elevation, future modeling work should use a constant level reservoir for the downstream boundary.

2.0 INTRODUCTION:

This report examines the hydraulic transients found in the preliminary treatment works of the 69th Street Wastewater Treatment (WWTP) Plant. The discharge of energy and momentum from pumps starting and stopping causes a velocity surges as those found in closed conduits. The sudden acceleration of the water forms a shallow water wave resulting in a transitory surge. This dynamic flow scours sediment from the channel and travels through the grit removal chambers. A numerical model of the influent channel represents the physical structure in order to gain a better understanding of the performance of the preliminary treatment works.

The 69th Street WWTP serves an area of 200 square miles of mixed use development. The average flow treated is approximately 70 million gallons per day (MGD) with wet weather peaks in excess of 350 MGD. Since it went into service in 1982, the plant has consistently exceeded the permitted treatment criteria. An effluent sharp crested weir measures the plant's flow. Figure 1 shows the daily average flow for 1995 as provided by City of Houston, Department of Public Works and Engineering. Significant rainfall events cause daily average peaks in excess of 200 MGD. When it rains, the infiltration and inflow into the wastewater collection system cause a sudden increase in flow. This surge of water flushes out the built-up solids. The reactors see a sudden buildup of inorganic matter that does not decay. The increase in solids challenges the treatment plant operators to control the solids in the reactors. The high level of mixed liquor suspended solid requires an increase in the rate of wasting sludge. How do the grit chambers work to minimize the impact of this first flush of solids?

The influent sample consists of a 24-hour composite sample drawn from the splitter box located upstream of the secondary reactors. This sampling point is after the preliminary treatment; therefore, since the wastewater does not contain rags or large particles, sampling problems associated with trash and grit is eliminated. There is no sampling program of the preliminary treatment system. The operators monitor the bar screens and grit removal systems for mechanical problems, spillage and dumpster capacity.

A twelve (12) foot diameter tunnel feeds the plant's pumping station that lifts the sewage up and into the preliminary treatment area. This pump station includes four (4) variable speed and four (4) fixed speed pumps. The variable speed pumps use a magnetic coupler and a logical controller to throttle the speed of the pumps. The system adjusts the speed of the pump to match the requirements for pumping the diurnal flow pattern thus eliminating the need for frequent starting of pumps. This report considers the impacts of wet weather surges that pass through the variable and fixed speed pump(s). When the wet weather induced surge reaches the pump station the fixed speed pumps are put into service to handle the peak. How do the surges generated by these pumps impact the operation of the preliminary treatment works?

2.1 MODELING GOALS:

This report describes a model used to identify the dynamic flow field in the preliminary treatment works of 69th Street Wastewater Treatment Plant. A numerical solution to the governing equations models the rapidly varied flow in the influent channel. The model answers the question of how quickly changes occur in the treatment works. Modeling the operation of the pumps demonstrates the impact on the channel flow.

The model predicts the hydraulic surge as the wave propagates through preliminary treatment works. This author believes the grit chambers store inorganic solids that are released when the wet weather peaks pass through the system. This model will predict the impact of starting a fixed speed pump on the dynamics of the grit chamber operation.

The other goal is to evaluate modeling strategies. The limitations of the solution technique as well as the theoretical basis of the model shall be identified. A sensitivity analysis will be performed to identify the important parameters.

2.2 GENERAL APPROACH:

A numerical model will be programmed into a spreadsheet using an explicit numerical method to solve for flow through the preliminary treatment works. The explicit scheme approximates the partial derivatives of time and space. Two sets of governing equations will be used to solve for the flow: the Method of Characteristics, and the Saint Venant. The primary purpose is estimate the unsteady flow at the grit chamber.

The Method of Characteristics guides and steers the calculations of the finite difference method used to solve the Saint Venant Equations for flow (Abbott, 1979). Furthermore, because the finite difference solution of the Saint Venant Equation is not satisfied at the boundaries, the method of characteristics solves for the boundary values. The two boundaries modeled are a known flow and a control weir. The influent channel is approximated by an ideal channel with a fixed cross sectional area and a constant slope. The Saint Venant Equation could approximate the actual geometry more closely; however, due to the averaging techniques used, a closely spaced grid with a small time interval is required.

3.0 HYDRAULIC SETTING AND CONCEPTUAL MODEL:

The 69th Street Sewerage system is modeled as a one-dimensional nearly horizontal flow. The flow is subcritical except at control structures such as weirs. A known discharge upstream boundary is coupled with a controlled discharge downstream boundary. The channel geometry is approximated for stability of the model.

The model uses a simple representation of a channel with constant cross section and friction. The input function of flow is varied over time to represent actual wet weather surges. The capacity of the influent pumps as shown on the City of Houston, Department of Public Works and Engineering, 1979 Design Drawings are listed in Table 1.

Table 1: Pump Capacity

Pump Number	Type of Pump	Capacity (gallons/minute)	Capacity (cubic feet/second)	Total Dynamic Head (feet)
P-201A	Variable	36,000	80.2	31
P-201B	Variable	36,000	80.2	31
P-201C	Variable	36,000	80.2	31
P-201D	Variable	36,000	80.2	31
P-202A	Fixed	52,000	115.8	31
P-202B	Fixed	52,000	115.8	31
P-203C	Fixed	52,000	115.8	31
P-203D	Fixed	52,000	115.8	31

Although actual pump start stopping data was not obtained, it is assumed that when the storm surge reaches the plant very rapid changes in pumping take place. The assumption includes the doubling of the variable speed flow in 60 seconds, the sudden starting of one (1) fixed speed pump, and the sudden starting of two (2) fixed speed pumps. These are believed to be common occurrences during wet weather events. The model assumes an initial condition of one variable speed pump running at a discharge of 75 cubic feet per second. The model uses one fourth (1/4) of the assumed flow rate, since all four (4) channels are normally in operation during peak demand.

The City of Houston, Department of Public Works and Engineering, 1979 Design Drawings detail the preliminary treatment works and the hydraulic profile, see Figures 2 and 3. The preliminary treatment system consists of the following:

- Entrance structure
- Four (4) Channels
- Four (4) Bar Screens
- Eight (8) Aerated Grit Removal Chambers

The entrance structure receives flow from four (4) force mains, and it routes the discharge onto the four (4) influent channels. A sluice gate located at the entrance to each channel is normally open. This gate is closed in order to drain the channel and the grit chambers for maintenance. Each channel is 6-feet wide which then expands to 12 feet wide and two feet deeper over a length of 8-feet. The bar screens are located in this expansion that is twelve (12) feet in length. The channel width is narrowed back too 6-feet over a 16-foot reach after the bar screen area. Each channel divides the flow into two (2) aerated grit chambers. The entrance to the grit chamber is a sudden expansion at the chamber wall.

Each aerated grit chamber is a rectangular unit twenty-one and a half (21.5) foot in width and twenty-five (25) feet in length. There is a slight bottom slope across the width. Coarse air bubble diffusers are located between a baffle wall and the side of the tank. The baffle wall runs the length of the tank. The air flow acts like a pump, and it creates a rolling velocity perpendicular to the flow through the tank. An auger the length of the tank moves the grit deposits to a sump. The solid-liquid slurry is pumped to a hydrocyclone. There is one (1) inclined-screw classifiers for four (4) grit chambers. The liquid is recycled to the influent channel upstream of the grit chamber. The classified grit is dropped into a roll-off dumpster. The de-gritted wastewater flows over a weir and onto the splitter box which routes the flow to the first stage reactors. A trough is located the width of the tank and near the weir. This trough triples the effective weir length and minimizes changes in the water surface elevation.

The model ignores the curvature off the channel as well as the bar screens. Also, the effluent weir in the grit chamber is approximated for stability. The trough is not modeled at all. The models approximate the channel as a constant width, depth, and slope. The effluent weir approximation should not impact the estimated flow rate. The water surface elevation is not accurately measured due to the approximation of the weir length. The model is intended to estimate the flow rate at the entrance to the aerated grit chamber.

4.0 MODEL DESIGN AND RESULTS:

Two techniques will be evaluated for the dynamic modeling of this system. Both methods are programmed into a computer spreadsheet, and are used to calculate the time variations in the flow rate. First, the method of characteristics is the basis for a finite difference scheme as presented by Stoker (1958). Then a solution of the Saint Venant equations is programmed into another spreadsheet.

4.1 THE METHOD OF CHARACTERISTICS:

The method of characteristics models rapidly varied dynamic flow. Stoker (1958) presents a mathematical proof of this method. An explicit finite difference scheme in a fixed rectangular grid of the spatial and time plane approximates the differential equations. The two sets of characteristic curves are solved to determine the characteristic at a future time step. The slope of the curve is equal to $u \pm c$ where c is the wave celerity defined by $c=\sqrt{gh}$, and u is velocity.

Governing Equations:

$$2\{(c+v)\, \partial/\partial x + \partial/\partial t\}c + \{(c+v)\, \partial/\partial x + \partial/\partial t\}v + E = 0$$

$$-2\{(-c+v)\, \partial/\partial x + \partial/\partial t\}c + \{(-c+v)\, \partial/\partial x + \partial/\partial t\}v + E = 0$$

C1 curve: $dx/dt = u + c$

C2 curve: $dx/dt = u - c$

where $c = \sqrt{(gh)}$

Along the C1 curve, $u + 2c + Et$ = constant, and along the C2 curve $u - 2c + Et$ = constant.

where $E = -gS + gS_f$

g = acceleration due to gravity

S = Physical Slope

S_f = Frictional Slope

These relationships provide the basis for a simple numerical solution that uses a the method of finite differences in a fixed rectangular grid. See Figure 4 below. The initial conditions are known. The solution for the celerity and velocity at point P is found by solving the following equations (Stoker 1958):

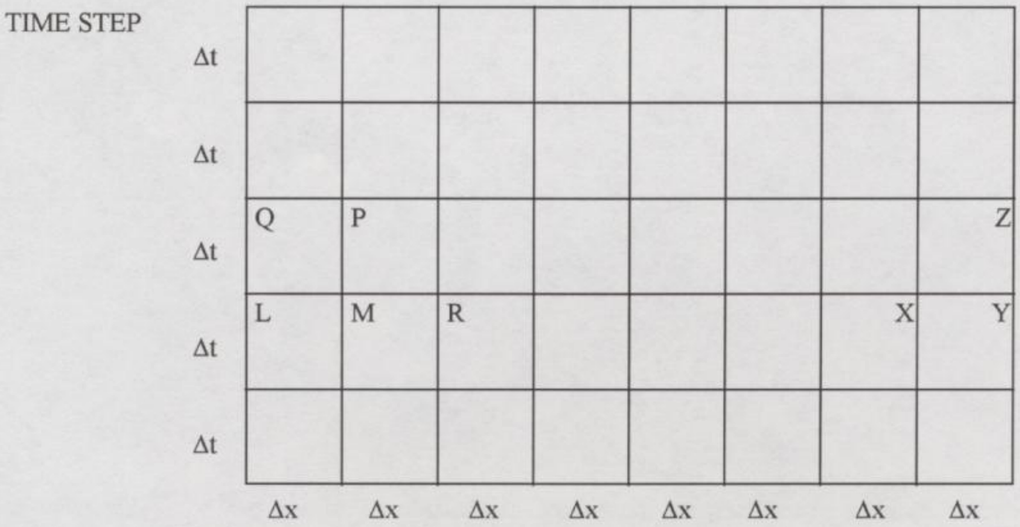

Figure 4, Grid for Method of Characteristics solution

by substituting difference quotients for the derivatives in the governing equations:

$$2\{(c_M+v_M)(c_M-c_L)/\Delta x + (c_P-c_M)/\Delta t\} + \{(c_M + v_M)(v_M-v_L)/\Delta x + (v_P-v_M)/\Delta t\}$$
$$+ E(v_M, c_M) = 0$$

$$-2\{(-c_M+v_M)(c_R-c_M)/\Delta x + (c_P-c_M)/\Delta t\} + \{(-c_M + v_M)(v_R-v_M)/\Delta x + (v_P-v_M)/\Delta t\}$$
$$+ E(v_M, c_M) = 0$$

The equations are solved to find the two unknowns vp and cp:

$$v_P = v_M + \Delta t/\Delta x\,[(c_M + v_M)(\tfrac{1}{2}v_L - \tfrac{1}{2}v_M + c_L - c_M)$$
$$- (c_M - v_M)(\tfrac{1}{2}v_M - \tfrac{1}{2}v_R - c_M + c_R) - \Delta x * E_M]$$

$$c_P = c_M + \tfrac{1}{2}\Delta t/\Delta x\,[(c_M + v_M)(\tfrac{1}{2}v_L - \tfrac{1}{2}v_M + c_L - c_M)$$
$$+ (c_M - v_M)(\tfrac{1}{2}v_M - \tfrac{1}{2}v_R - c_M + c_R)]$$

The results from the above equations determine both the depth H and flow rate q.

$H_P = c_P^2/g$

$q_P = v_P * H_P * b$; where b = channel width

The new values of depth and flow are loaded back into the initial values for the next set of calculations.

4.2 BOUNDARY CONDITIONS:

The upstream is a known flow boundary that is solved by using a modification of the method presented by J. J. Stoker, 1958. Stoker presents the following equation for the upstream boundary with a known head.

$v_Q = v_L + \Delta t \{ 1/\Delta x(c_L - v_L) (2c_L - 2c_M - v_L + v_M) - E_L\} + 2(c_Q - c_L)$

However, since $c_Q = \sqrt{gh}$ at point Q, v_Q cannot be solved directly. The $2c_Q$ is moved to the left hand side, resulting in the following equations:

$f(x) = v_Q - 2c_Q = v_L + \Delta t \{ 1/\Delta x(c_L - v_L) (2c_L - 2c_M - v_L + v_M) - E_L\} - 2c_L$

$v_Q = q /(h_Q*b)$

$c_Q = \sqrt{(h_Q * g)}$

The model interpolates values for velocity and celerity (Casey, 1992). The value of v_M and c_M is adjusted for the actual slope of the characteristic and the ratio of Δt to Δx. This procedure is performed at both boundaries. The value of h at point Q is solved by Newton's Method (Hoffman, 1992).

$f'(xi) = [f(\alpha) - f(xi)] / [x(i+1) - xi]$

or $x(i+1) = xi + [f(\alpha) - f(xi)] / f'(xi)$

$f(\alpha)$ = is the next approximation of the function.

where $f'(xi) = [q / hb - 2\sqrt{(h*g)}]\ dh = - q/ (b * h\hat{}2) - 2*[-½ \sqrt{(g / h)}]$

The first approximation is made by h = hl. Since the solution converges rapidly, the spreadsheet calculates four (4) iterations at each time step.

The downstream boundary is a sharp crested weir for which a depth to discharge relationship is established. A similar method is used with the forward characteristic to calculate the water surface elevation at the downstream boundary.

$v_Z = v_Y + \Delta t \{ 1/\Delta x[(c_Y + v_Y) (2c_X - 2c_Y + v_X - v_Y)] - E_Y\} + 2(c_Y - c_Z)$

$f(x) = v_Z + 2c_Z = v_Y + \Delta t \{ 1/\Delta x[(c_Y + v_Y)(2c_X - 2c_Y + v_X - v_Y)] - E_Y\} + 2c_Y$

Using the standard sharp crested weir equation q = L * 2/3 √(2g) y^3/2 a relationship between depth and discharge is formulated. Substituting q/A into the above equation:

$f(x) = L * 2/3 \sqrt{(2g)}\, y^{3/2} / (h*b) + 2 \sqrt{(g*h)} + Et$

where y = h - constant. The constant is the height of the weir above the channel bottom.

The derivative of the above equation is complicated by the relationship of h to y. Therefore, the secant method (Hoffman, 1992) is used to approximate the value of h. This method approximates the nonlinear function $f(x)$ with a linear function $g(x)$. The function g(x) is a secant to $f(x)$. Two initial estimates of x are required for the following equation:

$g'(x) = \{f[x(i)] - f[x(i-1)]\} / [x(i) - x(i-1)]$

where the secant line is given by

$\{f(\alpha) - f[x(i)]\}/[x(i+1)-x(i)] = g'[x(i)]$

solving for x(i+1) yields

$x(i+1) = x(i) + \{f(\alpha) - f[x(i)]\}/ g'[x(i)]$

This method does not converge as rapidly as the Newton method used for the upstream boundary. Eight iterations are performed for each time step. The above derivations of the boundary conditions is also applied to the Saint Venant solution described below.

4.3 SAINT VENANT EQUATION:

This method is used for calculation of the interior points within the grid. The boundary point shown as q cannot be calculated with the above equations since there is no forward curve to establish the l to p relationship. The method of characteristics described above solves for the boundary points. The Saint Venant Equation is solved for the interior points.

Saint Venant Governing Equations:

The continuity equation is expressed as follows:

$b(\partial H / \partial t) + \partial q / \partial x = i$ where i= inflow to the channel

and the momentum equation as:

$\partial q / \partial t + (\partial / \partial x)(q^2 / A) + gA(\partial H / \partial x + s_f - s) = 0$

momentum conservation law according to Abott (1979).

$$[u_j^{n+1} - (u_{j+1}{}^n + u_{j-1}{}^n)/2]/\Delta t + [(u^2/2 + gh)_{j+1}{}^n - (u^2/2 + gh)_{j-1}{}^n]/2\Delta x = 0$$

the mass law of the Lax scheme:

$$[h_j{}^{n+1} - (h_{j+1}{}^n + h_{j-1}{}^n)/2]/\Delta t + [(uh)_{j+1}{}^n - (uh)_{j-1}{}^n]/2\Delta x = 0$$

Wood (1994) describes the Lax-Wendroff explicit scheme using the mesh shown in Figure 4A. A system of equations with one unknown are developed. The q and H values are known, then the values of $H^{n+1/2}{}_{j+1/2}$ and $q^{n+1/2}{}_{j+1/2}$ are calculated using approximation of the form

$$\partial f / \partial t \cong 2/\Delta t\ [f^{n+1/2}{}_{j+1/2} - (f^n{}_{j+1} + f^n{}_j) / 2]$$

for the time derivatives. The space derivatives from the St. Venant continuity equation above $H^{n+1/2}{}_{j+1/2}$ is found from

$$½\ (b^n{}_{j+1} + b^n{}_j)\ [H^{n+1/2}{}_{j+1/2} - ½\ (H^n{}_{j+1} + H^n{}_j)]\ 2/\Delta t + 1/\Delta x\ (q^n{}_{j+1} - q^n{}_j) = ½\ (i^n{}_{j+1} + i^n{}_j)$$

when $i = 0$

$$H^{n+1/2}{}_{j+1/2} = ½\ (H^n{}_{j+1} + H^n{}_j)] + \Delta t/[\Delta x\ (b^n{}_{j+1} + b^n{}_j)]\ (q^n{}_{j+1} - q^n{}_j)$$

and $q^{n+1/2}{}_{j+1/2}$ is found from momentum equation

$$2/\Delta t\ [q^{n+1/2}{}_{j+1/2} - ½\ (q^n{}_{j+1} + q^n{}_j)] + 1/\Delta x\ [(q^2/A)^n{}_{j+1} - (q^2/A)^n{}_j]$$
$$+ g/2\ (A^n{}_{j+1} + A^n{}_j)\ [1/\Delta x\ (H^n{}_{j+1} - H^n{}_j) + ½\ [(s_f)^n{}_{j+1} + (s_f)^n{}_j - s] = 0$$

$$q^{n+1/2}{}_{j+1/2} = ½\ (q^n{}_{j+1} + q^n{}_j) + \Delta t/(2\Delta x)\ [(q^2/A)^n{}_j - (q^2/A)^n{}_{j+1}]$$
$$+ \Delta t\ g / 4\ (A^n{}_{j+1} + A^n{}_j)\ [1/\Delta x\ (H^n{}_j - H^n{}_{j+1}) - ½\ [(s_f)^n{}_{j+1} + (s_f)^n{}_j] + s]$$

The St. Venant equations are solved using the following form

$$\partial f/\partial t \cong (f^{n+1}{}_j - f^n{}_j) / \Delta t$$

$H^{n+1}{}_j$ is calculated by

$$1/\Delta t\ [b^n{}_j\ (H^{n+1}{}_j - H^n{}_j)] + 1/\Delta x\ (q^{n+½}{}_{j+½} - q^{n+½}{}_{j-½}) = ½\ i^n{}_j$$

$$H^{n+1}{}_j = H^n{}_j + \Delta t/(\Delta x\ b^n{}_j)\ (q^{n+½}{}_{j-½} - q^{n+½}{}_{j+½})$$

and $q^{n+1}{}_j$ is calculated by

$$1/\Delta t\ (q^{n+1}{}_j - q^n{}_j) + 1/\Delta x\ [(q^2/A)^{n+½}{}_{j+½} - (q^2/A)^{n+½}{}_{j-½}]$$
$$+ g/2\ (A^{n+½}{}_{j+½} + A^{n+½}{}_{j-½})\ \{1/\Delta x\ (H^{n+½}{}_{j+½} - H^{n+½}{}_{j-½}) + ½\ [(s_f)^{n+½}{}_{j+½} + (s_f)^{n+½}{}_{j-½}] - s\} = 0$$

$$q^{n+1}{}_j = q^n{}_j + \Delta t / \Delta x * [(q^2/A)^{n+½}{}_{j-½} - (q^2/A)^{n+½}{}_{j+½}]$$
$$+ \Delta t * g/2\ (A^{n+½}{}_{j+½} + A^{n+½}{}_{j-½})\ \{1/\Delta x\ (H^{n+½}{}_{j-½} - H^{n+½}{}_{j+½}) - ½\ [(s_f)^{n+½}{}_{j+½} + (s_f)^{n+½}{}_{j-½}] - s\}$$

The method is stable with the time step limited by

$$\Delta t/\Delta x = 1/\ [v + \sqrt{(gH)}\ ]$$

The $q^{n+½}_{j-½}$ is estimated form the average flow of q^{n+1}_j - q^n_j * 0.5. The $\Delta x_{j-½}$ term is found from the characteristic of H^n_j and q^{n+1}_j.

4.4 MODEL DESIGN:

Excel Spreadsheets solve the above equations. The calculations are performed on a series of worksheets that are part of one workbook. A macro copies the flow rate and water surface elevation to a separate sheet and then recalculates the worksheet. The macro is located on "Module1" and is implemented with the "Ctrl A" key combination. The "Ctrl D" combination is used on the Saint Venant Model. If over thirty iterations are to be saved the data is manually copied to another worksheet.

Figure 5 shows the first work sheet. This worksheet, "Sheet1," contains fields for the adjustment of the engineering parameters as follows:

- Time Step interval -- cell C1
- Reset to Initial Conditions -- cell E1
- Flow Rate -- cell G1
- Manning's "n"-- cell I1
- Weir Length -- cell G2

Cell C5 contains the flow rate for the upstream boundary. It includes an if statement that resets to the initial flow rate should the reset cell be set to 0. The same is true for the water surface elevations. When the reset cell is set to zero, then the sheet uses a pre-defined initial elevation for the boundary elevation. Other areas define the channel width, slope and bottom elevation. This sheet is the same for both models: The Method of Characteristics; and The Saint Venant Solution.

The method of characteristics model contains two additional calculations sheets. Sheet2 calculates the boundary conditions - see Figure 6. Sheet3 calculates the interior points on the grid - see Figure 7. When the spreadsheet is set to calculate, Sheet1 updates the values of flow and water surface elevation from Sheet2 and Sheet3. Then these updated values are used to calculate the next time step.

The Saint Venant Equation model uses three additional calculation sheets. Sheet2 calculates the 1/2 time step at 1/2 grid points - see Figure 8. Sheet3 calculates the boundary conditions as in the Method of Characteristics Workbook. Sheet4 calculates the full time step at full grid points - see Figure 9. When the sheet recalculates, the values of flow and water surface elevation update the values in Sheet1.

4.5 VERIFICATION AND SENSITIVITY ANALYSIS:

The above models contain ten (10) calculation points or nine (9) cells. The first test is a constant flow. The flow does approximate steady state conditions after numerous iterations. The number of iterations required will vary significantly with the chosen initial conditions. Figure 10 shows the results. Also, the model is tested with zero flow. The water surface approximates the weir elevation and the flow approaches zero at all points, see Figure 11.

A sensitivity analysis identifies the important variables. The analysis began when flow rate doubled at time equal to one. The sensitivity analysis included the following variables:

- Weir Length “L”
- Manning’s “n”
- Channel Width “W”
- time step “t”
- Change in Flow Rate

The models are very sensitive to the weir length, channel width and the time step chosen. The weir length and channel width will result in significant over or under estimation of the surge. The manning’s n value within the range of 0.01 to 0.03 has little impact on the model results. The values shown in the following tables list the parameters used for the sensitivity analysis.

The weir analysis shows a significant over or under estimation just after the surge reaches the weir. Over estimation was significant for weir lengths greater than 17 feet or channel widths to weir length ratios less than 0.35. Also, there is an under estimation when the ratio of channel length to weir length is greater than 0.4. The Method of Characteristics Solution has a significantly less error that the solution of the Saint Venant Equation. The flow rate over the weir is plotted on figures 12 and 13. Furthermore, it appears the magnitude of the surge impacts the error associated with the weir length.

Table 2: Input Parameter for Weir Length

Analysis	Weir Length (feet)	Manning's n	Channel Width (feet)	time step (seconds)	ratio Channel/Weir
Weir	12	0.013	6	1	0.5
Weir	15	0.013	6	1	0.4
Weir	16	0.013	6	1	0.38
Weir	17	0.013	6	1	0.35
Weir	18	0.013	6	1	0.33
Weir	21	0.013	6	1	0.29

The variation in the friction factor or Manning's "n" tended to flatten out the slope of the surge at the higher values of n. The expected range of this value is between 0.010 and 0.020 for the channel being modeled. The results are not significantly different within this range of values. Therefore, the final model uses a manning's "n" value of 0.013. This value should provide adequate results for this modeling exercise. The flow rate over the weir is plotted on figures 14 and 15.

Table 3: Input Parameter for Variation in Manning's "n"

Analysis	Weir Length (feet)	Manning's "n" for MOC - St Venant		Channel Width (feet)	time step (seconds)
Mannings "n"	16	0.010	0.010	6	1
Mannings "n"	16	0.020	0.011	6	1
Mannings "n"	16	0.030	0.013	6	1
Mannings "n"	16	0.040	0.014	6	1
Mannings "n"	16	0.050	0.015	6	1
Mannings "n"	16	0.060	0.020	6	1
Mannings "n"	16	0.100	0.025	6	1

The analysis of the channel width shows similar results as the weir analysis, however, since the ratio of "Width to Weir" is over a larger range the results are more significant. See figures 16 for the flow rate over the weir.

Table 4: Input Parameters for Variation in Channel Width

Analysis	Weir Length (feet)	Manning's n	Channel Width (feet)	time step (seconds)	ratio Width/Weir
Width	16	0.013	2	1	0.13
Width	16	0.013	3	1	0.19
Width	16	0.013	4	1	0.25
Width	16	0.013	5	1	0.31
Width	16	0.013	6	1	0.38
Width	16	0.013	8	1	0.5
Width	16	0.013	10	1	0.63
Width	16	0.013	20	1	1.25

The variation in the time step had a profound effect on the models' results, see figures 17 and 18. The Courant Number gauges the time step for an exact solution:

$$\text{Courant Number} = (\Delta t/\Delta x)\,[v + \sqrt{(gH)}]$$

The model was not stable for a Courant Number greater than one. The time step of 1.35 seconds, Courant Number of 0.994, produced a very sharp front, see Figures 19 and 20. This is the most accurate representation of the idealized model. Courant Numbers of 0.35 and larger produced an output with a wave front. The time steps associated with the Courant Number of 0.07 and 0.007 produced no noticeable front at the weir. The Courant Number is a good indicator of the degree of numerical dispersion generated by the model. Courant Numbers approaching one will minimize numerical dispersion. The Saint Venant Model predicts a steeper wave front for Courant Numbers of 0.35 and 0.70. Apparently the Method of Characteristics is more susceptible to numerical dispersion than the Saint Venant Model.

Table 5: Input Parameters for Variation in time step

Analysis	Weir Length (feet)	Manning's n	Channel Width (feet)	time step (seconds)	Courant Number
time step	16	0.013	6	0.01	0.007
time step	16	0.013	6	0.1	0.07
time step	16	0.013	6	0.5	0.35
time step	16	0.013	6	1	0.70
time step	16	0.013	6	1.35	0.994

4.6 RESULTS

The following input functions simulate both the sudden starting of pump(s), and the operation of a variable speed pump:

Scenario 1:

at $t <= 0$: $q = 18.75$ cubic feet per second

at $t>0$: $q = q_o + 28.95 = 47.7$ cubic feet per second

Scenario 2:

at $t <= 0$: $q = 18.75$ cubic feet per second

at $t>0$: $q = q_o + 57.9 = 76.65$

Scenario 3:

at $t <= 0$: $q = 18.75$ cubic feet per second

at $t>0$: $q = q_o * (1 + t/60)$ and $t > 90$ $q = q_o * (2.5 - (t-90)/60)$ end at $t = 180$

The wave for the sudden starting of pumps travels through the channel very quickly. Figures 21 and 22 show the results. This is an extreme condition for the channel as well as the model. The starting of the fixed speed pump(s) changes the treatment parameters quickly. The following tables show the flow over the weir at the time steps associated with this front. The Courant Number for the analysis were 0.9. The sensitivity of the Method of Characteristics model is shown by the lower values of the flow gradient.

Table 6: Scenario 1 Wave Front

Time Step	Saint Venant flow (cfs)	Flow Gradient (cfs per second)	MOC flow (cfs)	Flow Gradient (CFAs per second)
10.8	18.95	0	18.75	0
12.0	23.95	4.2	23.38	3.7
13.2	38.60	12.2	32.60	7.7
14.4	52.37	11.5	41.31	7.3

Table 7: Scenario 2 Wave Front

Time Step	Saint Venant flow (cfs)	Flow Gradient (cfs per second)	MOC flow (cfs)	Flow Gradient (cfs per second)
10.8	18.95	0	18.75	0
12.0	27.23	6.9	27.88	7.6
13.2	58.90	26.4	50.39	18.8
14.4	85.30	22.0	71.66	17.7

Scenario 3 demonstrates that both models are extremely stable for gradually varied flow, see figures 23 and 24. A complex input equation could model a wide range of flows.

5.0 LIMITATIONS:

These models are only valid for the influent channel as described above. These models quantify the flow and the magnitude of the surge that reaches the grit chamber. The calculation of the water surface elevation is not accurate due to the adjustment made to the weir length. Therefore, the figures show the calculated flow only. Also, the models assume the waves travel in one direction without reflection. The actual channel generates a complex system of waves that we represent with a single wave.

The sudden discharge of the pumps at full capacity is not realistic, since pump systems require a finite amount of time to build momentum. The motor does not instantly reach full speed. Also, the elasticity of the force main dissipates the surge. However, for time steps greater than one second, the sudden surge into the channel is reasonable.

The model does not include the effects of the bar screen or the associated expansion in the channel. The model ignores the head losses at the bar screens and the associated disturbance to the wave. The expansion of the channel minimizes the bar screens impact on the water surface profile; however, since the model quantifies the flow, the bar screens impact on the wave propagation is of concern.

The model does not attempt to describe the complex flow field in the aerated grit chamber. The ninety (90) degree turns into the grit chamber and the sudden expansion are not modeled. The expansion probably will flatten out the surge. Also, the pumping action of the aerated grit chamber creates a rolling velocity perpendicular to the direction of flow. The rotational acceleration may impact the surge. Also, the entrained air could dampen the impact of the surge as it travels through the grit removal chamber.

6.0 CONCLUSIONS:

The model demonstrates that rapidly varied flow travels quickly through the preliminary treatment works. The wave velocity is about fifteen feet per second. The waves travel quickly from the preliminary treatment to the reactors and onto the effluent weir. The procedure described in this report could model the entire plant. A plant model requires development of a numerical representations for the grit chamber, reactors, clarifies, and filters. Also, procedures for recirculation of the flow are needed.

The sensitivity analysis showed that the wide channel tends to flatten the slope of the wave. The bar screen area is a source of potential error. The 20-foot grid spacing does not allow for the modeling of the actual width and depth of the channel. The Courant condition, $\Delta t/\Delta x <= 1/[v + \sqrt{(gH)}]$, requires adjustment of Δt for the change in Δx. Therefore, a closer grid spacing would require many more calculations. Decreasing the grid spacing from twenty (20) feet to two (2) foot would require one tenth of the time step. The number of iterations would increase by a factor of one hundred. The Excel Spreadsheet is quite capable of performing these calculations, but it would require more computational time.

The Method of Characteristics is valuable part of an explicit hydraulic model, and the procedure provides a viable technique for the calculation of the interior points between boundaries. The choice of a control weir boundary presented problems. A better choice may have been a constant elevation reservoir, since the long weir tends to minimize elevation changes in the grit chamber. The Method of Characteristics is an excellent solution for the rapidly varied flow problem described in this report. Chandhry, 1987, warns under his Section 12.7 METHOD OF CHARACTERISTICS, "This method is not suitable for systems having numerous geometrical changes, and it fails because of the convergence of the characteristic curves whenever a bore or shock forms." He includes the procedure for calculation of the boundaries in the explicit models he presents. The Method of Characteristics is very sensitive to the time step and the associated Courant Number. Therefore, this model requires adjustment of the time step in order to minimize numerical dispersion. The Lax-Wendroff explicit solution of the Saint Venant equations exhibits less numerical dispersion. Also, because this solution should be more stable for changes in channel geometry, it could be expended to represent the actual channel with a constant elevation downstream boundary. However, due to time restraints this project does not include this expanded model.

ACKNOWLEDGMENTS

I want to express my appreciation to Dr. Theodore Cleveland for his guidance and support, during his classes and research consultation. I also express my appreciation to Dr. K. H. Wang for teaching "Hydraulics of Open Channels", serving on my review committee and taking the time to critique my work. Also, I appreciate Dr. M. T. Garrett for sharing his experiences in wastewater research while with the City of Houston.

I would like to thank the City of Houston, Department of Public Works and Engineering, for there wonderful tuition reimbursement program that provided funding for this project and my course work. There were many people within the Department that have provided support, guidance and encouragement that I would like to mention. First Mr. Herb Fain for his strong support and encouragement throughout the program. Mr. Dave Peters, I thank you for introducing me to the University of Houston's Masters' Program. My current supervisor Mr. Doug Bernard and our Deputy Director Ms. Hilda Scott for their patience and support. The entire staff of the Wastewater Operation Division, but most of all Ms. Teresa Battenfield, Ms. Thien Nguyen, Mr. Zaki Ahmad and Mr. Gurdip Hyare. They provided data and access to the 69th Street Wastewater Treatment Facility.

I thank my wife and daughter for their encouragement and support through the years. Thank you Tina and Christine for the love, patience and encouragement that made this project possible.

REFERENCES:

Abbott, M. B. 1979. Computational Hydraulics, Elements of the Theory of Free Surface Flows. Pitman, London. 324pp

Casey, T. J. 1992. Water and Wastewater Engineering Hydraulics. Oxford University Press, New York, New York. 270pp

Chaudhry, M. H. 1987. Applied Hydraulic Transients. Van Nostrand Reinhold, New York, New York. 521pp

City of Houston, Department of Public Works and Engineering, 1979. Drawing Number 19219, "69th Street Wastewater Treatment Plant, Lift Station and Preliminary Treatment Facilities", unpublished, Houston, Texas. 159 Sheets

City of Houston, Department of Public Works and Engineering, 1996. "Effluent Data for 1995", unpublished, Houston, Texas. 1 diskette

Hoffman, J. D. 1992. Numerical Methods for Engineers and Scientists McGraw-Hill, New York, New York. 825pp

Stoker, J. J. 1958. Water Waves, The Mathematical Theory with Applications. Interscience, New York, New York. 567pp

Wood, W. L. 1993. Introduction to Numerical Methods for Water Resources. Oxford University Press, New York, New York. 255pp

Figure 1

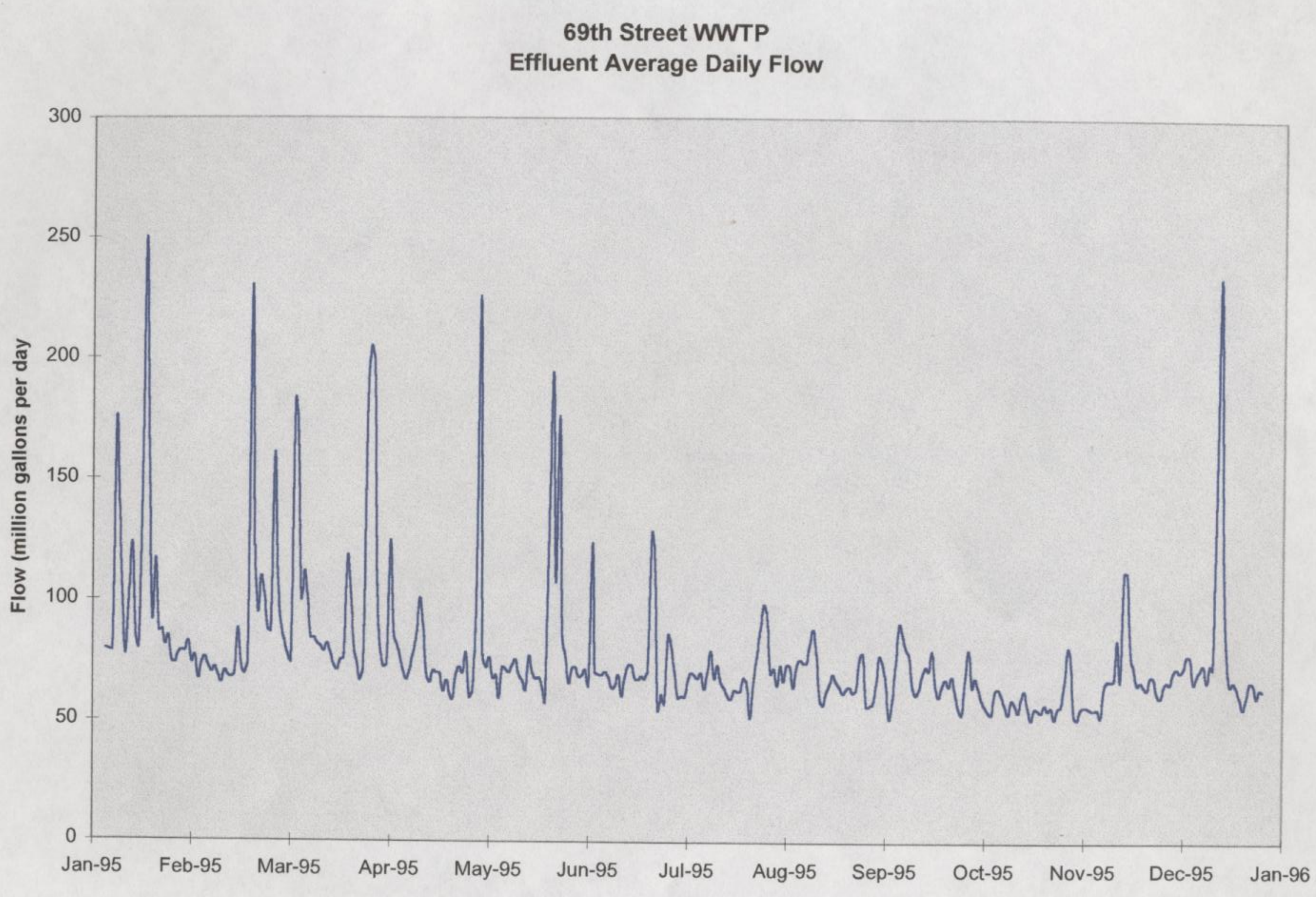

12/7/96

69DUMP.XLW

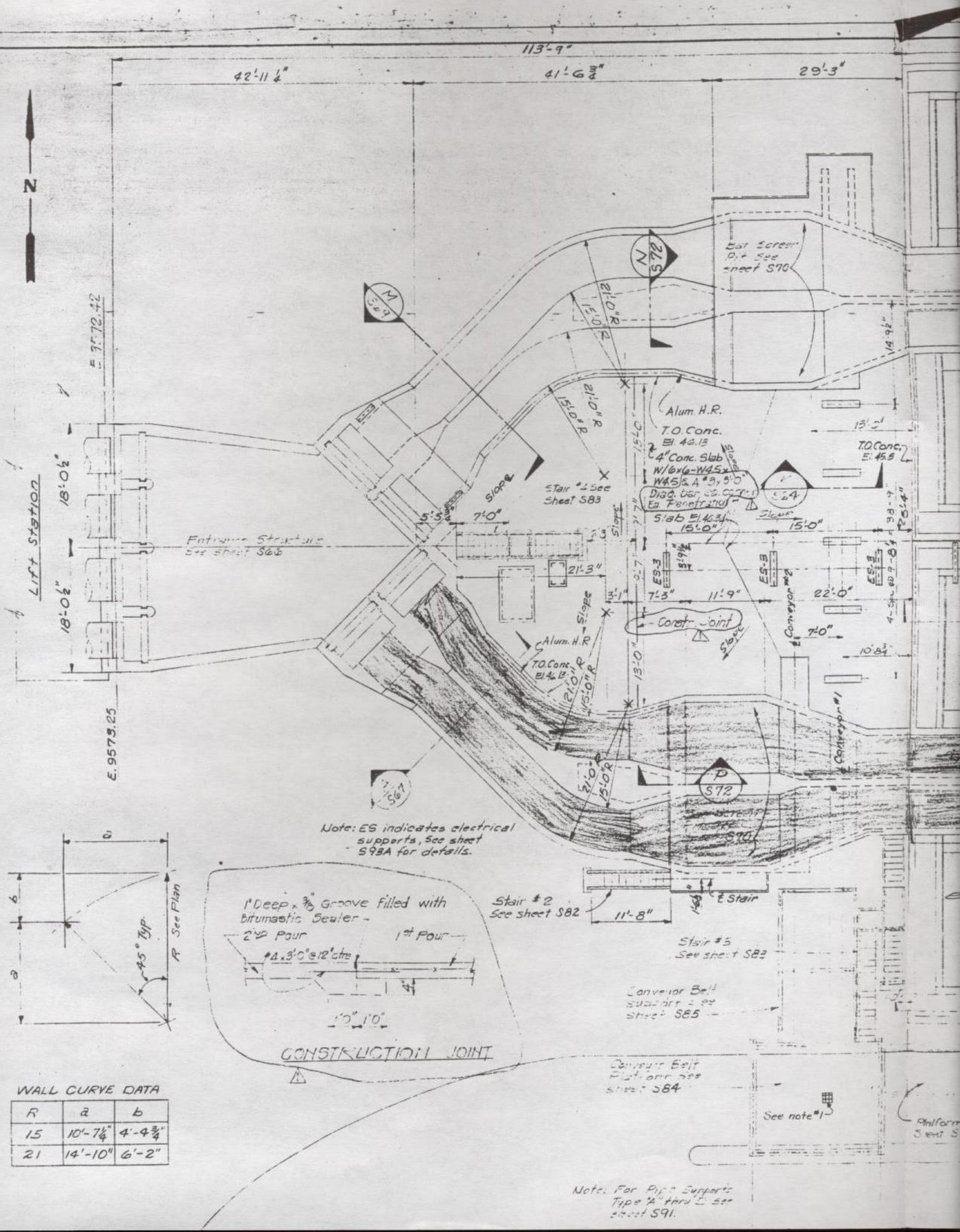

WALL CURVE DATA

R	a	b
15	10'-7 1/4"	4'-4 3/4"
21	14'-10"	6'-2"

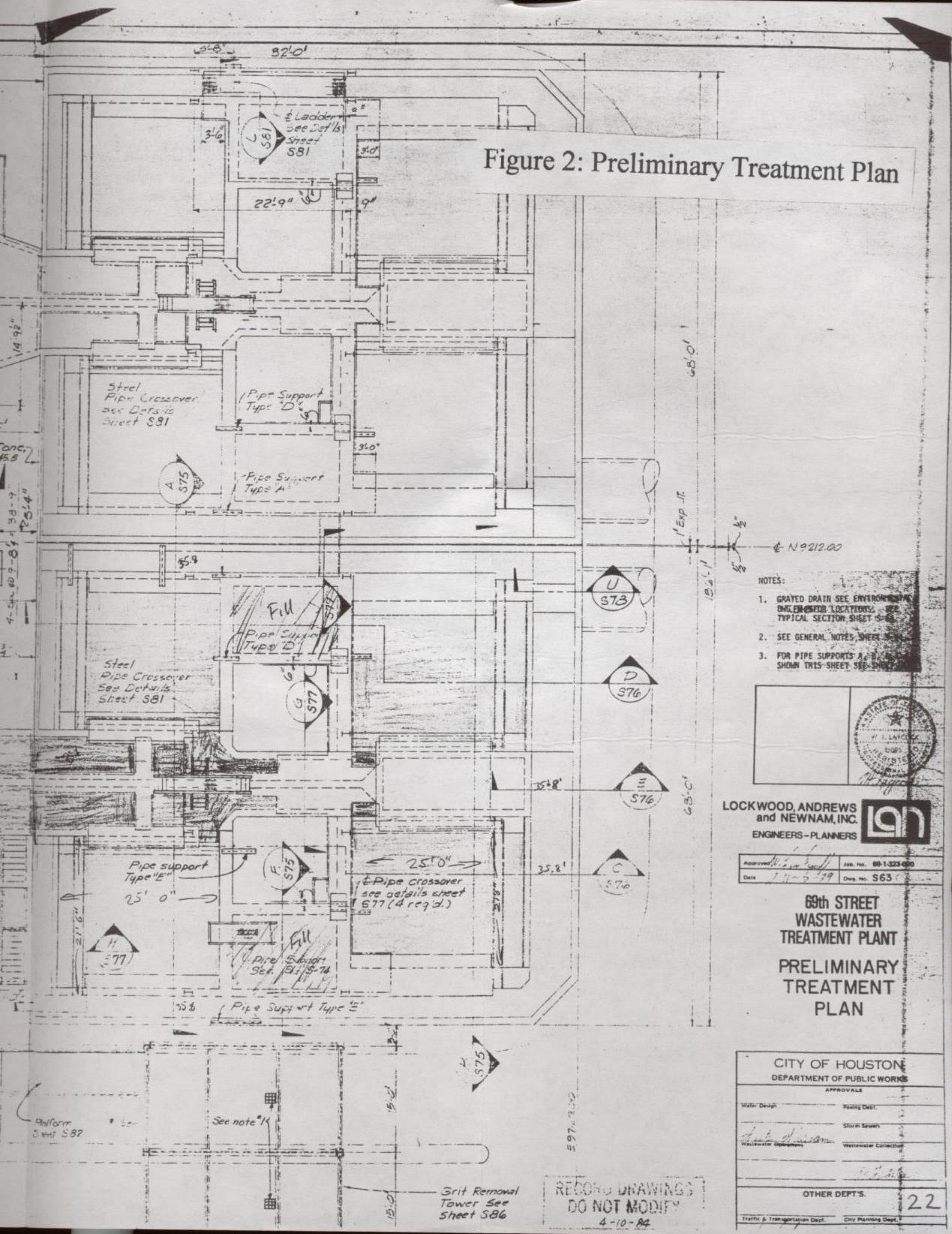

Figure 2: Preliminary Treatment Plan

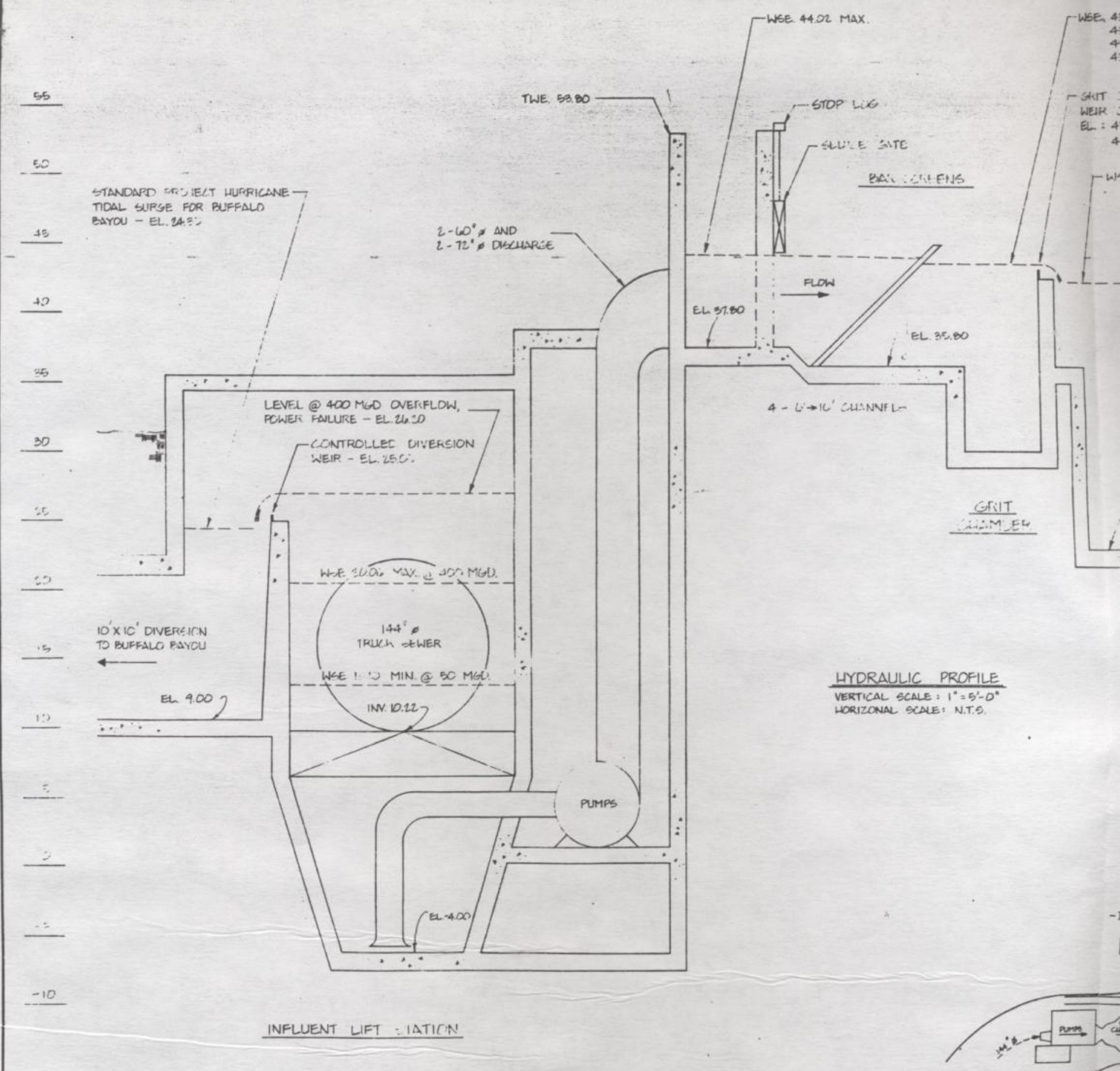

WSE. - WATER SURFACE ELEVATION
TWE. - TOP OF WALL ELEVATION
MAX. - MAXIMUM INFLUENT FLOW - 4?? MGD
DES. - DESIGN INFLUENT FLOW - 229 MGD
AVG. - AVERAGE INFLUENT FLOW - 116 MGD
MIN. - MINIMUM INFLUENT FLOW - 62 MGD

FLOW PATH

OPEN FLOW
CLOSED FLOW

Figure 3: Hydraulic Profile I

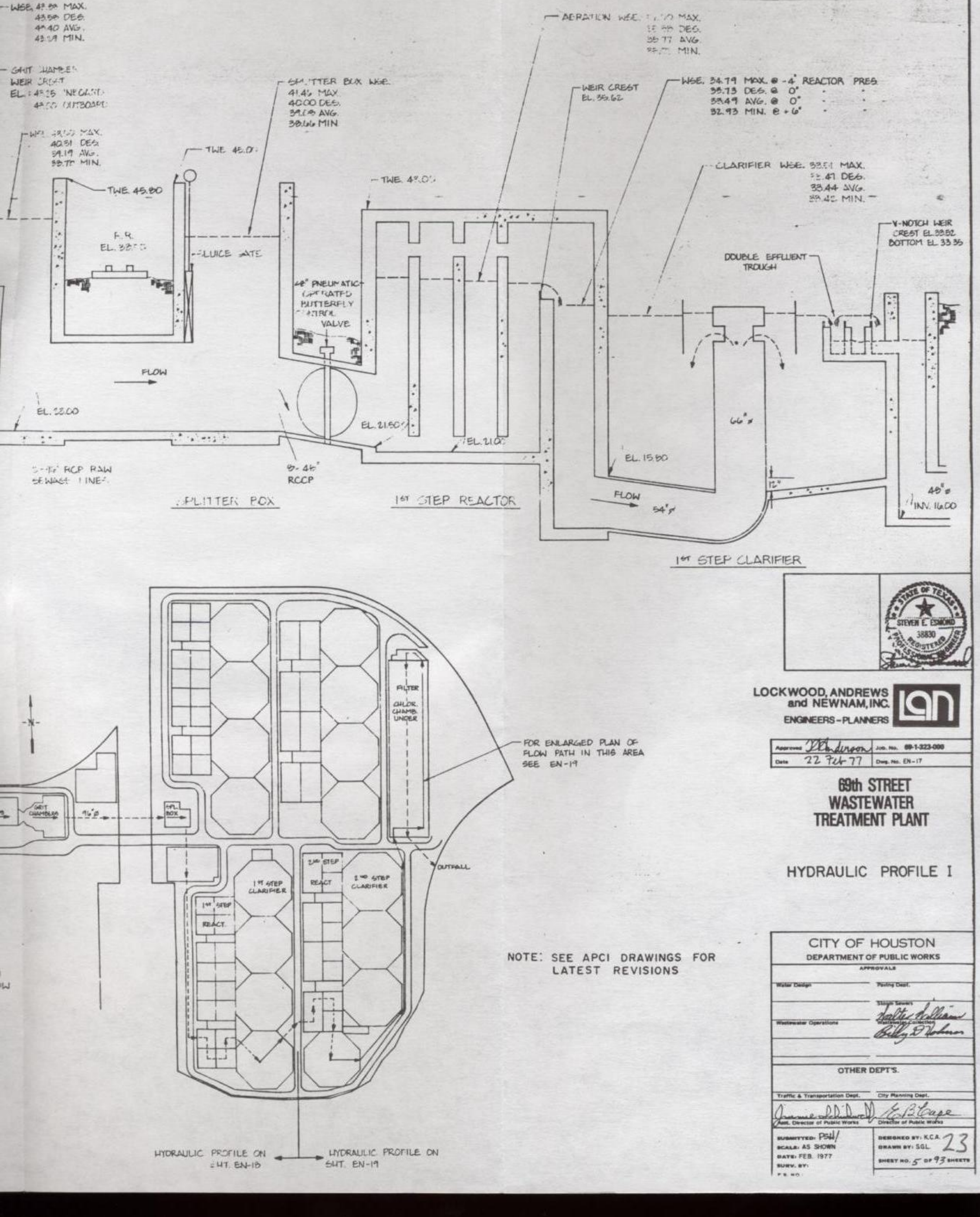

Figure 5
Sheet1 of Method of Characteristics Model

	A	B	C	D	E	F	G	H	I	J	K	L	M	N	O	P	Q	R
1		time step	1.35	59	1	q=	37.5	n=	0.013									
2				60	81	L=	16											
3		initial	81												wave			
4	j	plant flow	q (cfs)	v	WS ELEV	bottom	h	S	b	AREA	v	c	dx/dt	delta x	t (sec)	Sf	E	dh/dx
5	1	75	37.5	43.3652739	43.58349	37.8	5.783491	0	6	34.70095	1.080662	13.64655	14.72722	20	1.35803	3.61E-05	0.001161	28.37377
6	2	75	37.50537		43.58269	37.8	5.782695	0	6	34.69617	1.080966	13.64561	14.72658	20	1.358089	3.61E-05	0.001162	28.37219
7	3	75	37.50543		43.58197	37.8	5.781968	0	6	34.69181	1.081103	13.64476	14.72586	20	1.358155	3.61E-05	0.001162	28.37061
8	4	75	37.50545		43.58124	37.8	5.78124	0	6	34.68744	1.08124	13.6439	14.72514	20	1.358222	3.61E-05	0.001163	28.36904
9	5	75	37.50545		43.58051	37.8	5.780513	0	6	34.68308	1.081376	13.64304	14.72442	20	1.358288	3.61E-05	0.001163	28.36745
10	6	75	37.50543		43.57979	37.8	5.779785	0	6	34.67871	1.081511	13.64218	14.72369	20	1.358355	3.61E-05	0.001163	28.36587
11	7	75	37.5054		43.57906	37.8	5.779058	0	6	34.67435	1.081647	13.64132	14.72297	20	1.358422	3.61E-05	0.001164	28.36429
12	8	75	37.50537		43.57833	37.8	5.77833	0	6	34.66998	1.081782	13.64046	14.72224	20	1.358488	3.62E-05	0.001164	28.36271
13	9	75	37.50533		43.5776	37.8	5.777602	0	6	34.66561	1.081918	13.6396	14.72152	20	1.358555	3.62E-05	0.001164	28.36112
14	10	75	37.50512		43.57687	37.8	5.776872	0	6	34.66123	1.082048	13.63874	14.72079	20	1.358623	3.62E-05	0.001165	28.35953
15			WS ELEV				0.00662											
16			43.58349															
17			43.58269										Courant Number		0.993653			
18			43.58197															
19			43.58124															
20			43.58051															
21			43.57979															
22			43.57906															
23			43.57833															
24			43.5776															
25			43.57687															

Figure 6
Sheet2 of Method of Characteristics Model

	A	B	C	D	E	F	G	H	I	J	K	L	M	N	O	P	Q	R	S	T	U
1				dt	1.35		THETA	0.0675													
2				dx	20																
3	Solves for new y at pump discharge (2q)												t=n+1								
4	q	Y0	Y1	V0	V1	C0	C1	Vs	Cs	Ys	Sf (s)	dh/dx	y	q/A	Sf	C	dh/dy	delta	-q/(y*y*b)	-(g/y)^0.5	
5	37.5	5.783491	5.782695	1.080662	1.080966	13.64655	13.64561	1.08092	13.64576	5.782816	3.61E-05	-26.2124	5.783491	1.080662	3.61E-05	13.64655	-26.2124	2.67E-06	-0.18685	2.35957	-2.54642
6	37.5											-26.2124	5.78349	1.080662	3.61E-05	13.64655	-26.2124	-1.5E-13	-0.18685	2.35957	-2.54642
7													5.78349	1.080662	3.61E-05	13.64655	-26.2124	-3.6E-15	-0.18685	2.35957	-2.54642
8													5.78349	1.080662	3.61E-05	13.64655	-26.2124	0	-0.18685	2.35957	-2.54642
9													43.58349								
10	Solves for new q at the overflow weir																				
11		Y10	Y9	V10	V9	C10	C9	Vr	Cr	Yr		dh/dx	y	h	q	Sf	h^3/2	delta	H^3/2	g(x)	
12		5.776872	5.777602	1.082048	1.081918	13.63874	13.6396	1.081918	13.6396	5.777597	3.62E-05	28.35953	5.776872	0.576872	37.50512	3.62E-05	28.35953	1.31E-06	12.68322		
13												28.35953	5.776872	0.576872	37.50512	3.62E-05	28.35953	1.25E-06	12.68322	4.98719	
14												28.35953	5.776872	0.576872	37.50515	3.62E-05	28.35953	-1.8E-13	12.68323	4.98719	
15												28.35953	5.776872	0.576872	37.50515	3.62E-05	28.35953	0	12.68323	5	
16												28.35953	5.776872	0.576872	37.50515	3.62E-05	28.35953	0	12.68323	0	
17												28.35953	5.776872	0.576872	37.50515	3.62E-05	28.35953	0	12.68323	0	
18												28.35953	5.776872	0.576872	37.50515	3.62E-05	28.35953	0	12.68323	0	
19												28.35953	5.776872	0.576872	37.50515	3.62E-05	28.35953	0	12.68323	0	
20												28.35953	5.776872	0.576872	37.50515	3.62E-05	28.35953	0	12.68323	0	
21												28.35953	5.776872	0.576872	37.50515	3.62E-05	28.35953	0	12.68323	0	
22												28.35953	5.776872	0.576872	37.50515	3.62E-05	28.35953	0	12.68323	0	
23																					
24																					
25																					
26																					
27													5.481695	0.281695	18.49534						

Figure 7
Sheet3 of Method of Characteristics Model

	A	B	C	D	E	F	G	H	I	J	K	L	M
1				dt/dx	0.0675								
2													
3		j	cm+vm	vl-vm+cl-c	cm-vm	vm-vr-cm	dx*Em	delta v	v(t+1)	c(t+1)	y(t+1)	h(t+1)	q(t+1)
4													
5		1											
6		2	14.72658	0.000788	12.56465	-0.00093	0.023238	6.45E-07	1.080967	13.64561	5.782694	43.58269	37.50539
7		3	14.72586	0.000789	12.56365	-0.00093	0.023245	8.84E-07	1.081104	13.64475	5.781967	43.58197	37.50546
8		4	14.72514	0.00079	12.56266	-0.00093	0.023252	1.04E-06	1.081241	13.6439	5.78124	43.58124	37.50549
9		5	14.72442	0.00079	12.56166	-0.00093	0.023259	1.06E-06	1.081377	13.64304	5.780513	43.58051	37.50548
10		6	14.72369	0.000791	12.56067	-0.00093	0.023267	9.56E-07	1.081512	13.64218	5.779786	43.57979	37.50546
11		7	14.72297	0.000791	12.55967	-0.00093	0.023274	8.02E-07	1.081648	13.64132	5.779058	43.57906	37.50543
12		8	14.72224	0.000791	12.55868	-0.00093	0.023281	7.07E-07	1.081783	13.64046	5.77833	43.57833	37.50539
13		9	14.72152	0.000792	12.55769	-0.00093	0.023288	6.79E-07	1.081918	13.6396	5.777602	43.5776	37.50536
14		10											

Figure 8
Sheet2 of Saint Venant Model

	A	B	C	D	E	F	G	H	I	J	K	L	M	N
1		dt =	1							9:22 AM				
2														
3	j	b	dx	v	H	y	area	R	q	H1/2	delta q^2/	delta(h,Sf)	"k+l	q1/2
4		ft	ft	ft/s	ft				cfs					
5	1	6	20	1.077168	43.60225	5.802254	34.81352	1.977535	37.5	43.60022	-0.00408	0.024419	0.020344	37.55243
6	2	6	20	1.079667	43.59873	5.798729	34.79238	1.977125	37.56417	43.59754	0.000344	-0.00447	-0.00413	37.55281
7	3	6	20	1.079716	43.59623	5.79623	34.77738	1.976834	37.54971	43.59485	-0.0006	0.002068	0.001464	37.55233
8	4	6	20	1.080293	43.59349	5.793494	34.76097	1.976516	37.55202	43.59216	-0.00035	0.000551	0.000199	37.55113
9	5	6	20	1.080731	43.59081	5.79081	34.74486	1.976204	37.54984	43.58947	-0.0004	0.000837	0.000433	37.54964
10	6	6	20	1.081198	43.58811	5.788112	34.72867	1.975889	37.54858	43.58677	-0.00043	0.000605	0.000174	37.54837
11	7	6	20	1.081679	43.58542	5.78542	34.71252	1.975575	37.54781	43.58407	-0.00042	0.000755	0.000332	37.54767
12	8	6	20	1.082157	43.58272	5.78272	34.69632	1.975261	37.54687	43.58138	-0.00082	-0.00164	-0.00245	37.54772
13	9	6	20	1.082838	43.5801	5.780102	34.68061	1.974955	37.55347	43.5787	0.001489	0.012353	0.013842	37.54849
14	10	6	20	1.082337	43.57698	5.776982	34.66189	1.974591	37.51583					

Figure 9
Sheet4 of Saint Venant Model

	A	B	C	D	E	F	G	H	I	J	K	L	M
1	j	b	h1/2	y1/2	A1/2	R	q1/2	sf1/2	j	h_full	q_full, 1st	q_full, 2nd	q_full
2	1	6											
3	1.5	6	43.60022	5.800224	34.80135	1.977299	37.55243	0.000133					
4	2.5	6	43.59754	5.79754	34.78524	1.976987	37.55281	0.000133	2	43.59873	-0.00098	0.001513	37.56471
5	3.5	6	43.59485	5.794852	34.76911	1.976674	37.55233	0.000133	3	43.59623	-0.00089	0.001524	37.55034
6	4.5	6	43.59216	5.792161	34.75297	1.976361	37.55113	0.000133	4	43.5935	-0.00081	0.001563	37.55277
7	5.5	6	43.58947	5.789466	34.7368	1.976047	37.54964	0.000133	5	43.59082	-0.00078	0.001601	37.55065
8	6.5	6	43.58677	5.78677	34.72062	1.975733	37.54837	0.000134	6	43.58812	-0.00081	0.001555	37.54932
9	7.5	6	43.58407	5.784074	34.70445	1.975418	37.54767	0.000134	7	43.58543	-0.00087	0.001317	37.54826
10	8.5	6	43.58138	5.781384	34.6883	1.975105	37.54772	0.000134	8	43.58272	-0.00095	0.000882	37.5468
11	9.5	6	43.5787	5.778699	34.67219	1.974791	37.54849	0.000134	9	43.5801	-0.00103	0.000387	37.55283
12	10	6											

Figure 10

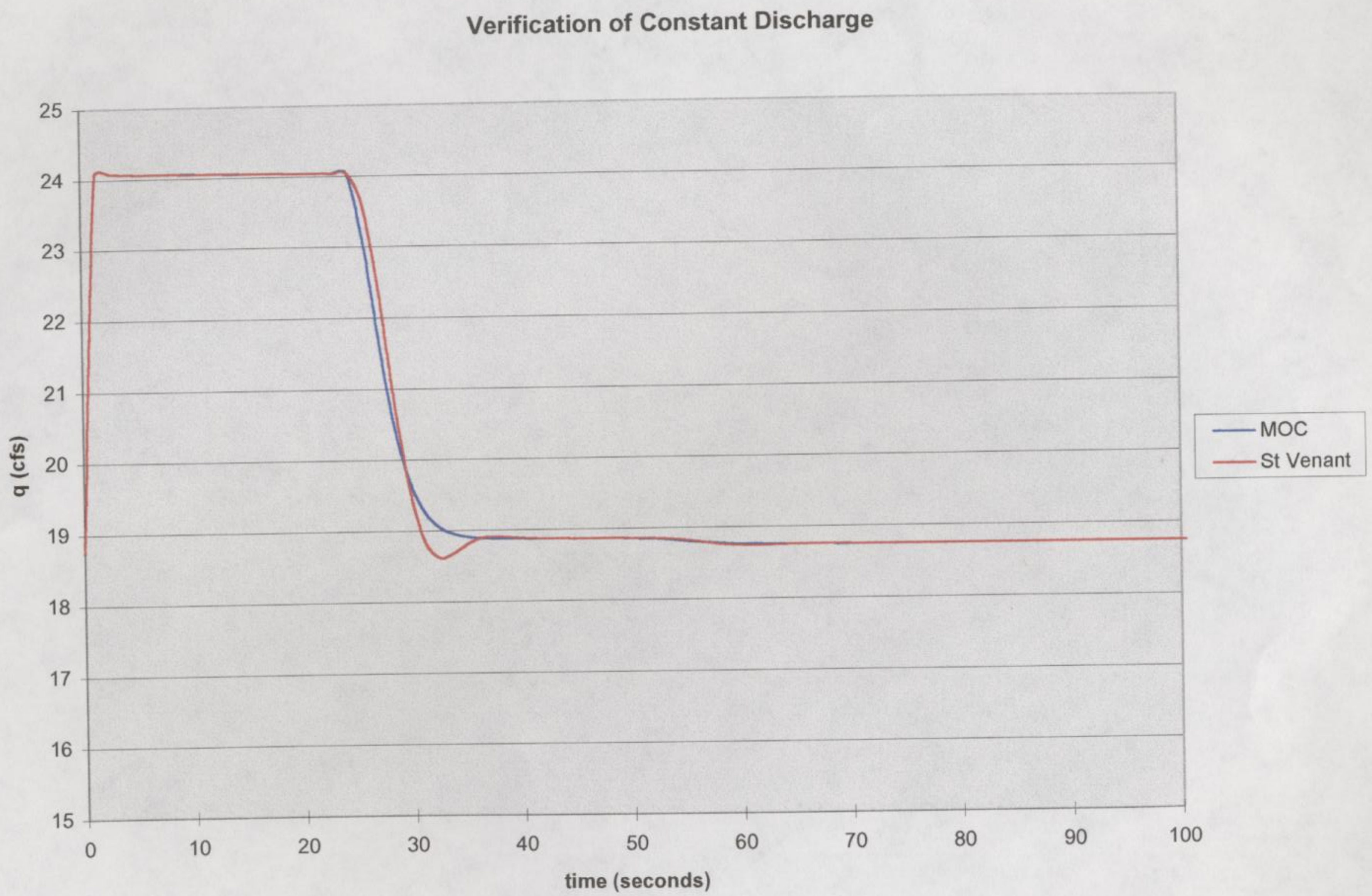
Verification of Constant Discharge
25
24
23
22
21
20
19
18
17
16
15
q (cfs)
0
10
20
30
40
50
60
70
80
90
100
time (seconds)
MOC
St Venant

Figure 11

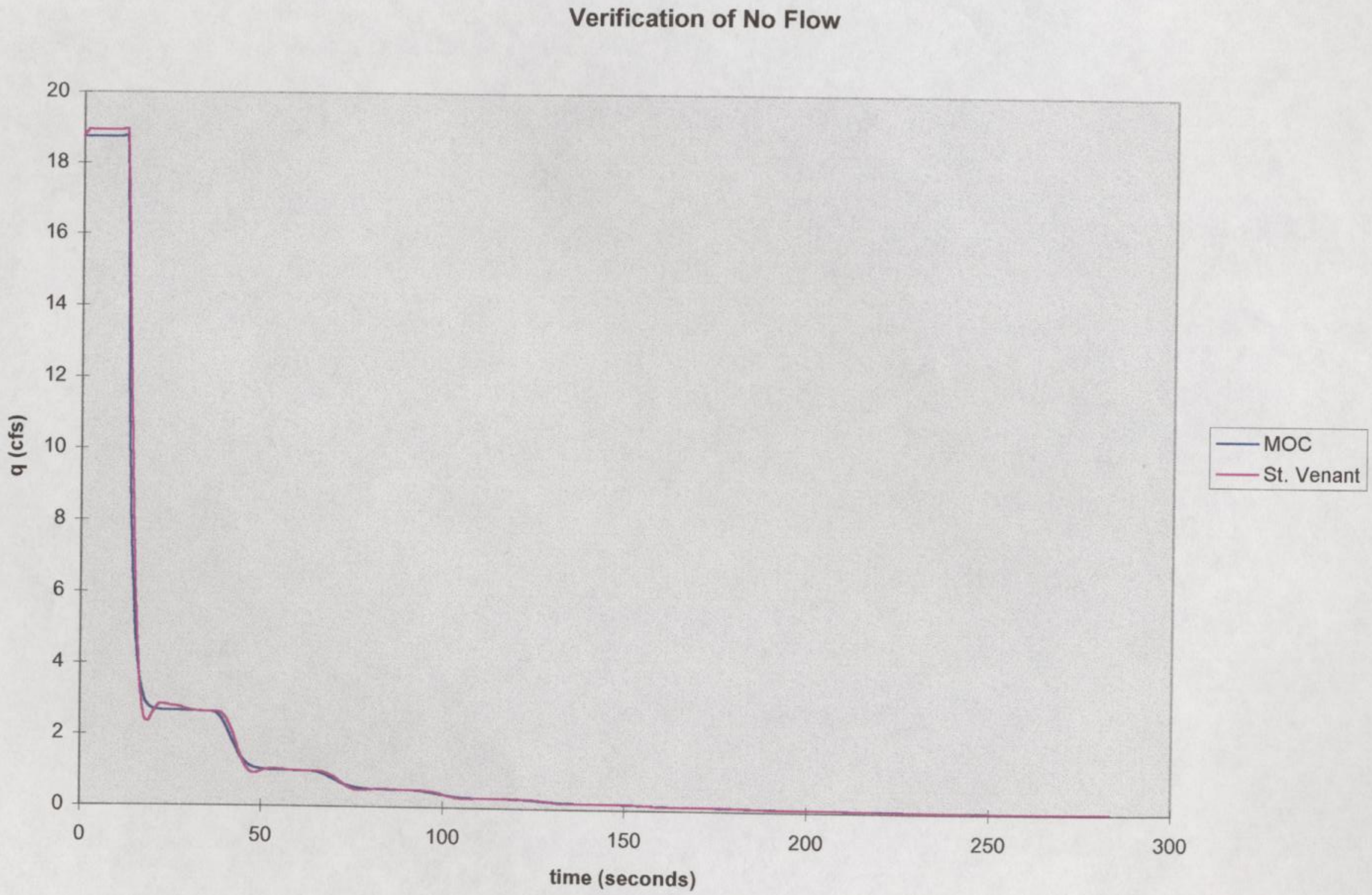
Verification of No Flow
20
18
16
14
12
10
8
6
4
2
0
q (cfs)
0
50
100
150
200
250
300
time (seconds)
MOC
St. Venant

Figure 12

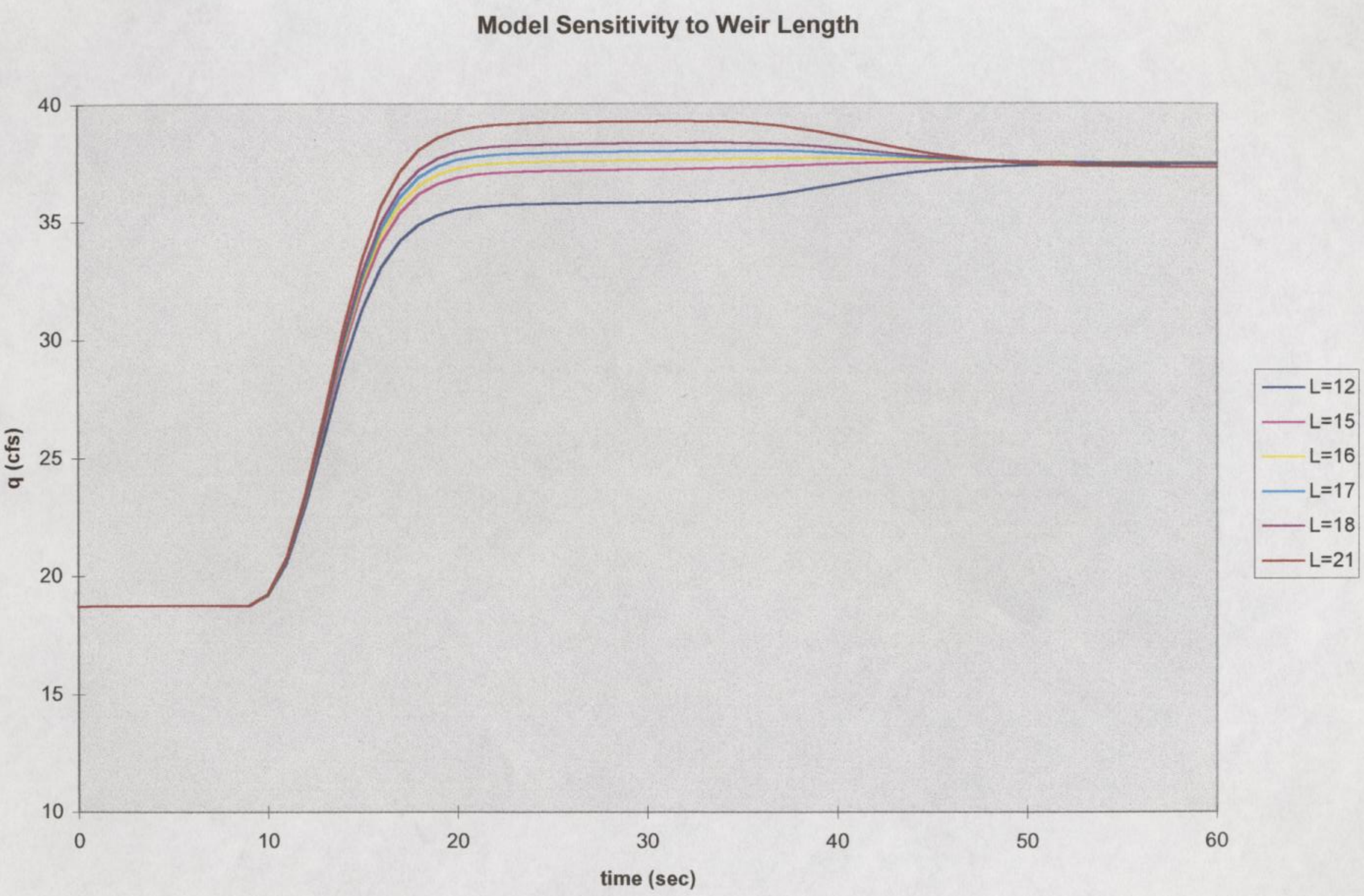
Model Sensitivity to Weir Length
q (cfs)
40
35
30
25
20
15
10
0
10
20
30
40
50
60
time (sec)
L=12
L=15
L=16
L=17
L=18
L=21

Figure 13

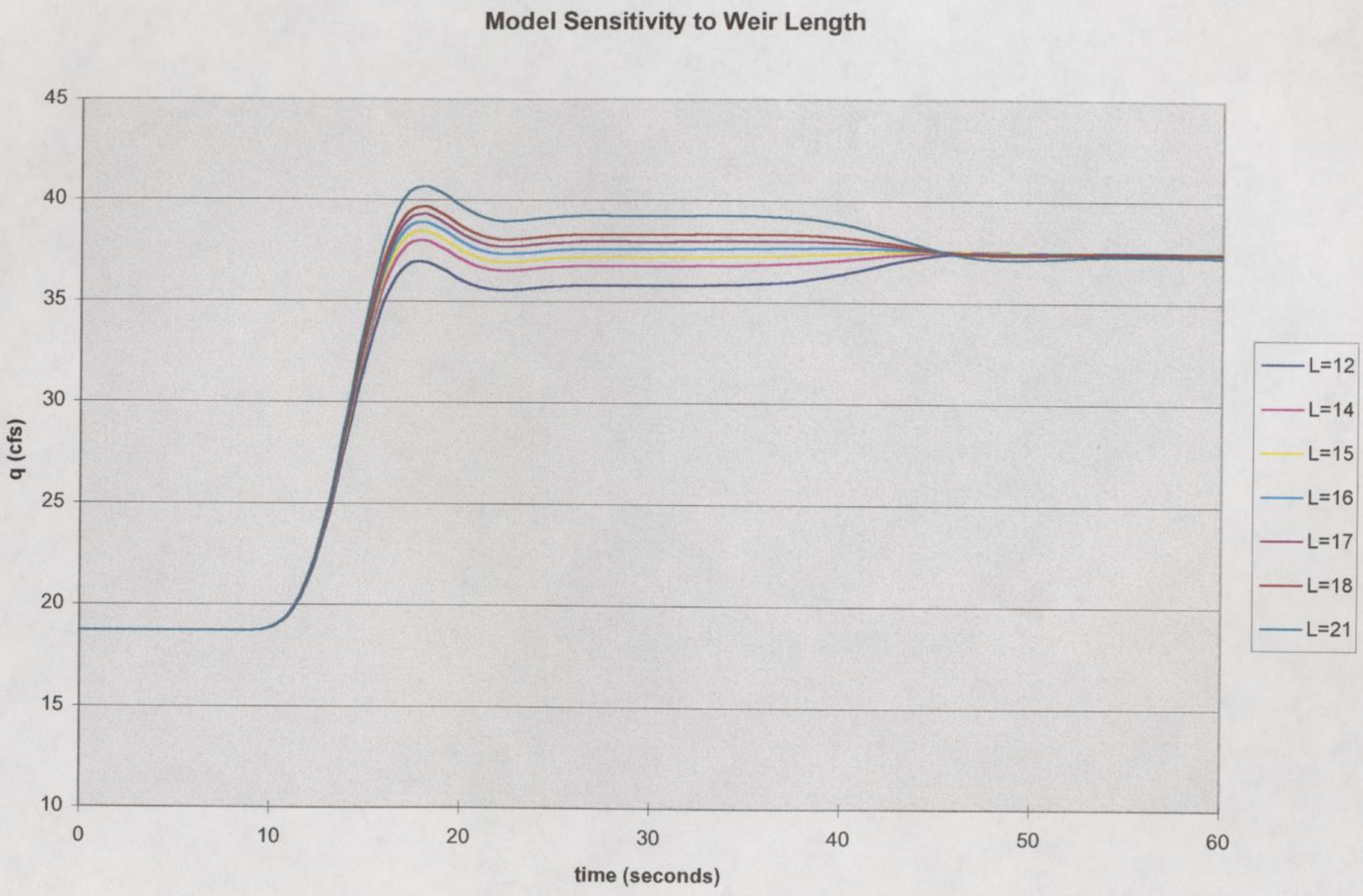
Model Sensitivity to Weir Length
45
40
35
30
25
20
15
10
q (cfs)
0
10
20
30
40
50
60
time (seconds)
L=12
L=14
L=15
L=16
L=17
L=18
L=21

Figure 14

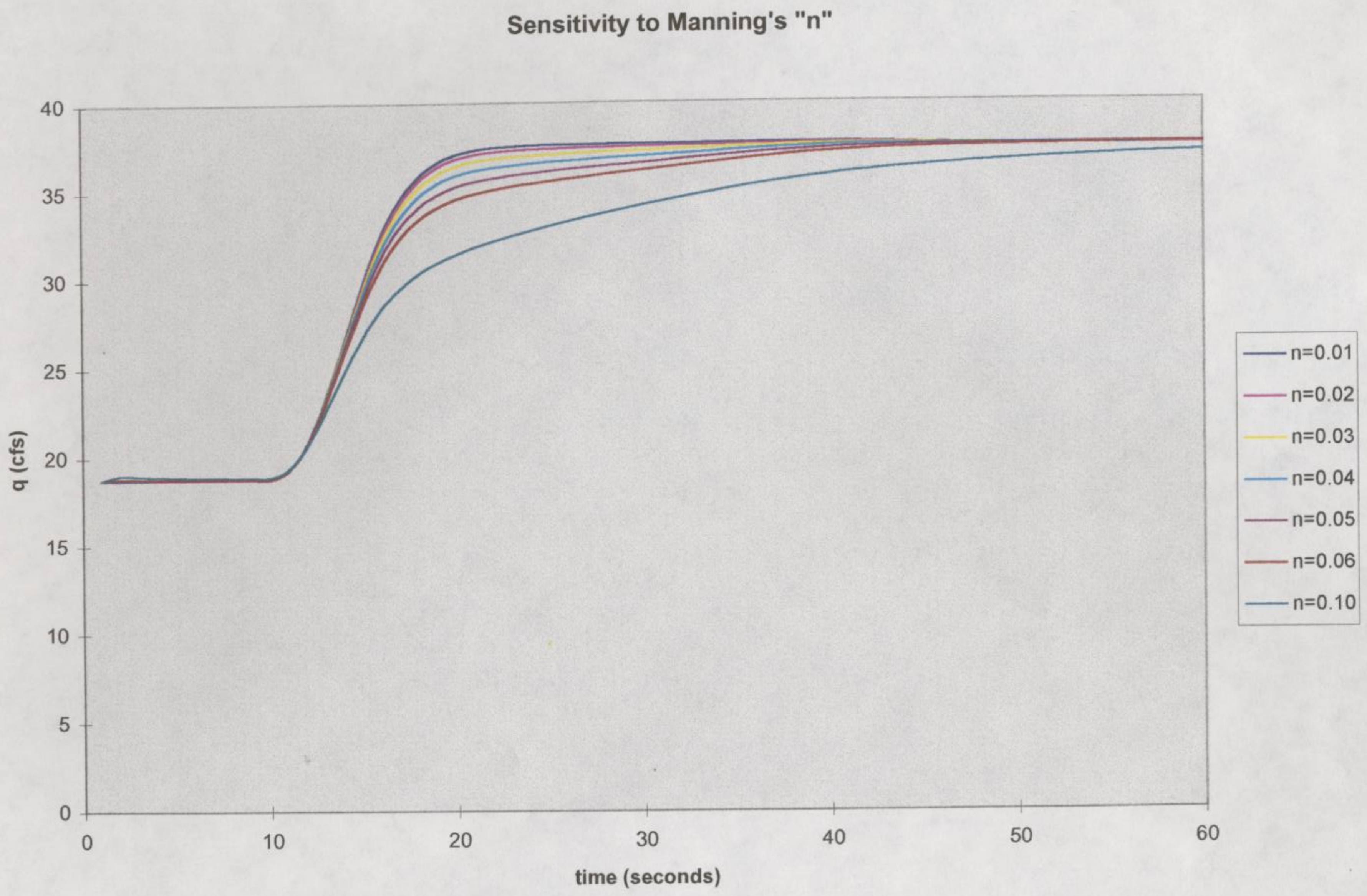
Sensitivity to Manning's "n"
40
35
30
25
20
15
10
5
0
q (cfs)
0
10
20
30
40
50
60
time (seconds)
n=0.01
n=0.02
n=0.03
n=0.04
n=0.05
n=0.06
n=0.10

Figure 15

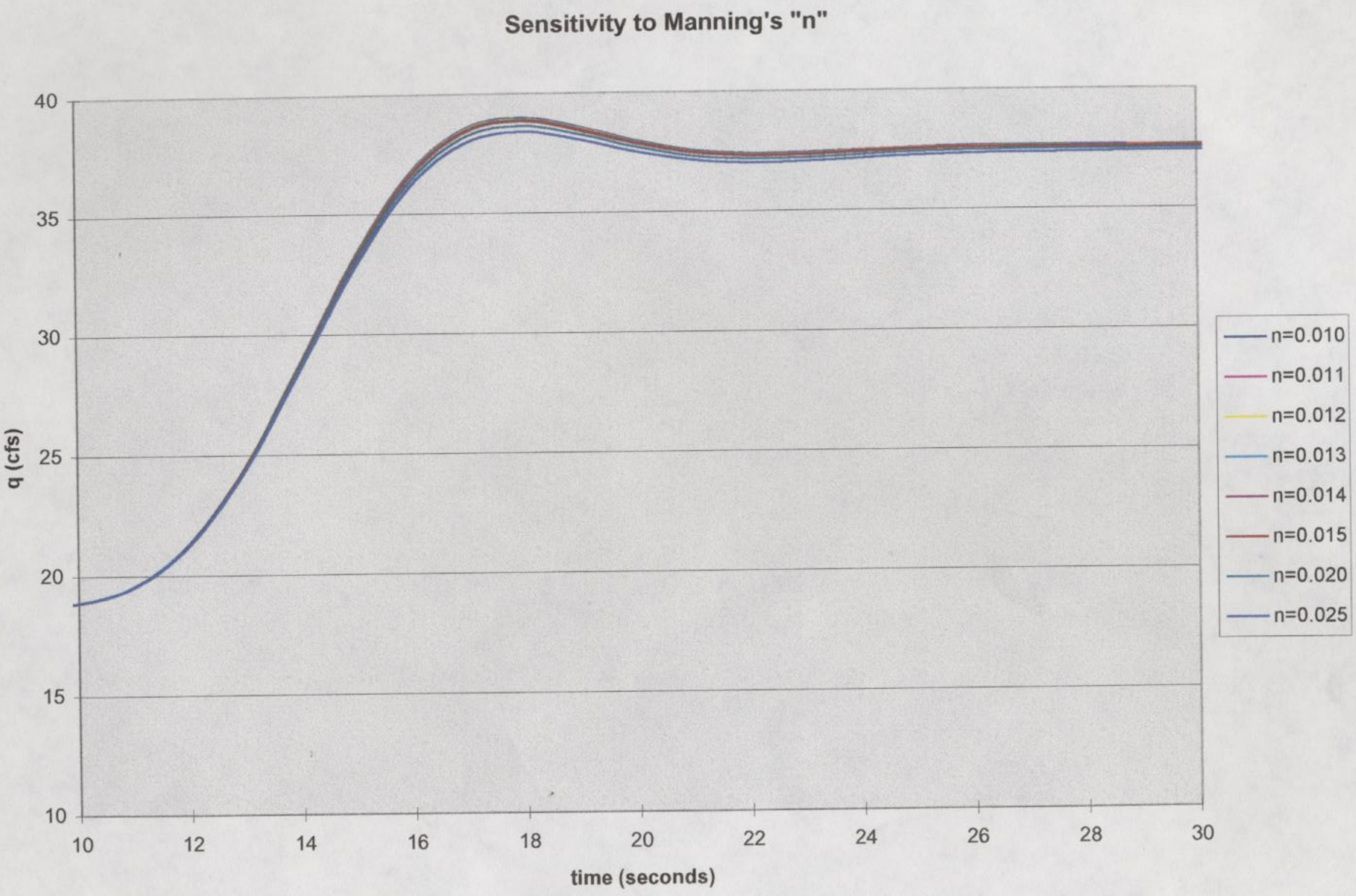
Sensitivity to Manning's "n"
q (cfs)
40
35
30
25
20
15
10
10
12
14
16
18
20
22
24
26
28
30
time (seconds)
n=0.010
n=0.011
n=0.012
n=0.013
n=0.014
n=0.015
n=0.020
n=0.025

Figure 16

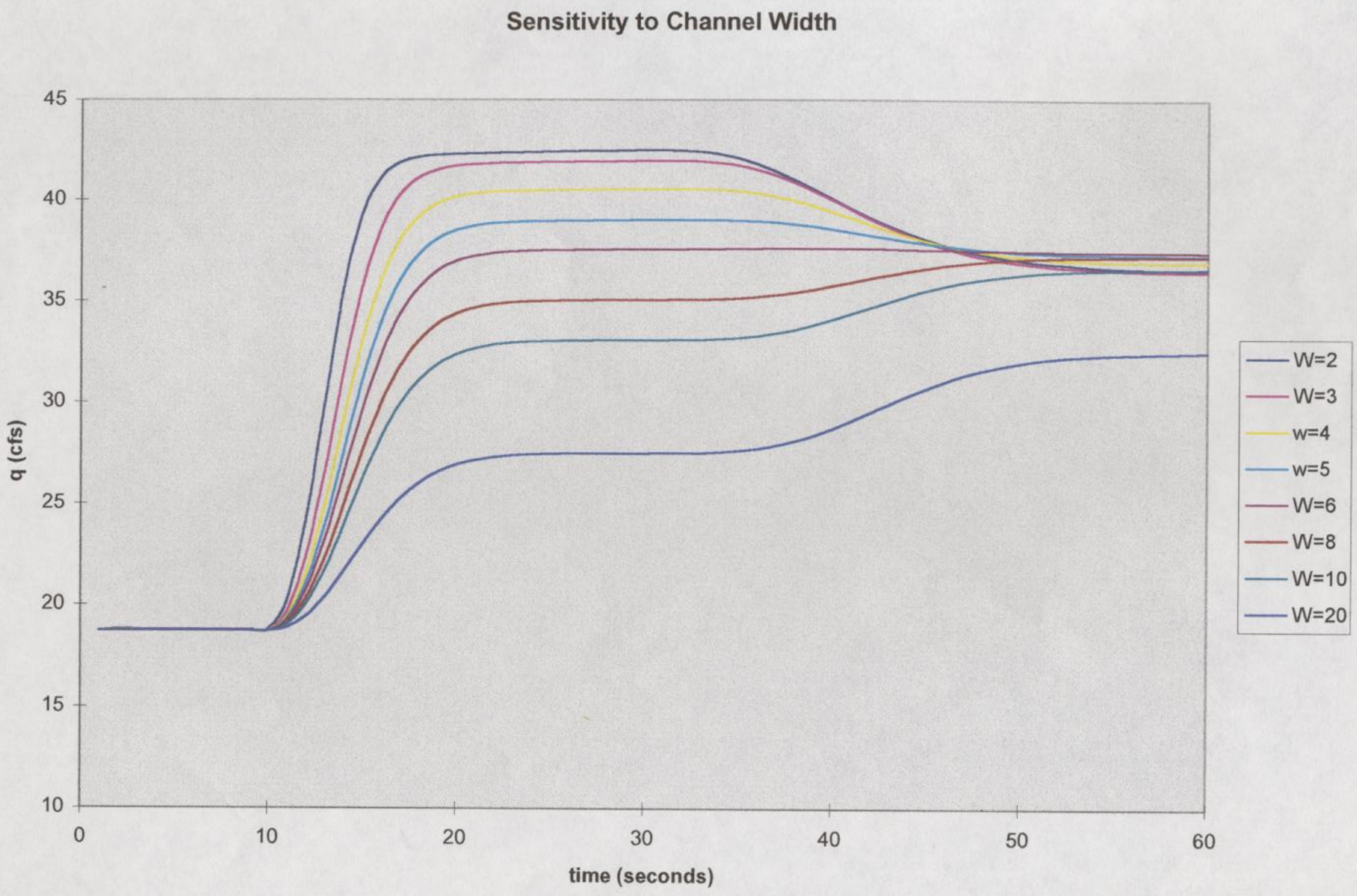

Sensitivity to Channel Width
45
40
35
30
25
20
15
10
q (cfs)
0
10
20
30
40
50
60
time (seconds)
W=2
W=3
w=4
w=5
W=6
W=8
W=10
W=20

Figure 17

Metod of Characteristics

Sensitivity to Delta t

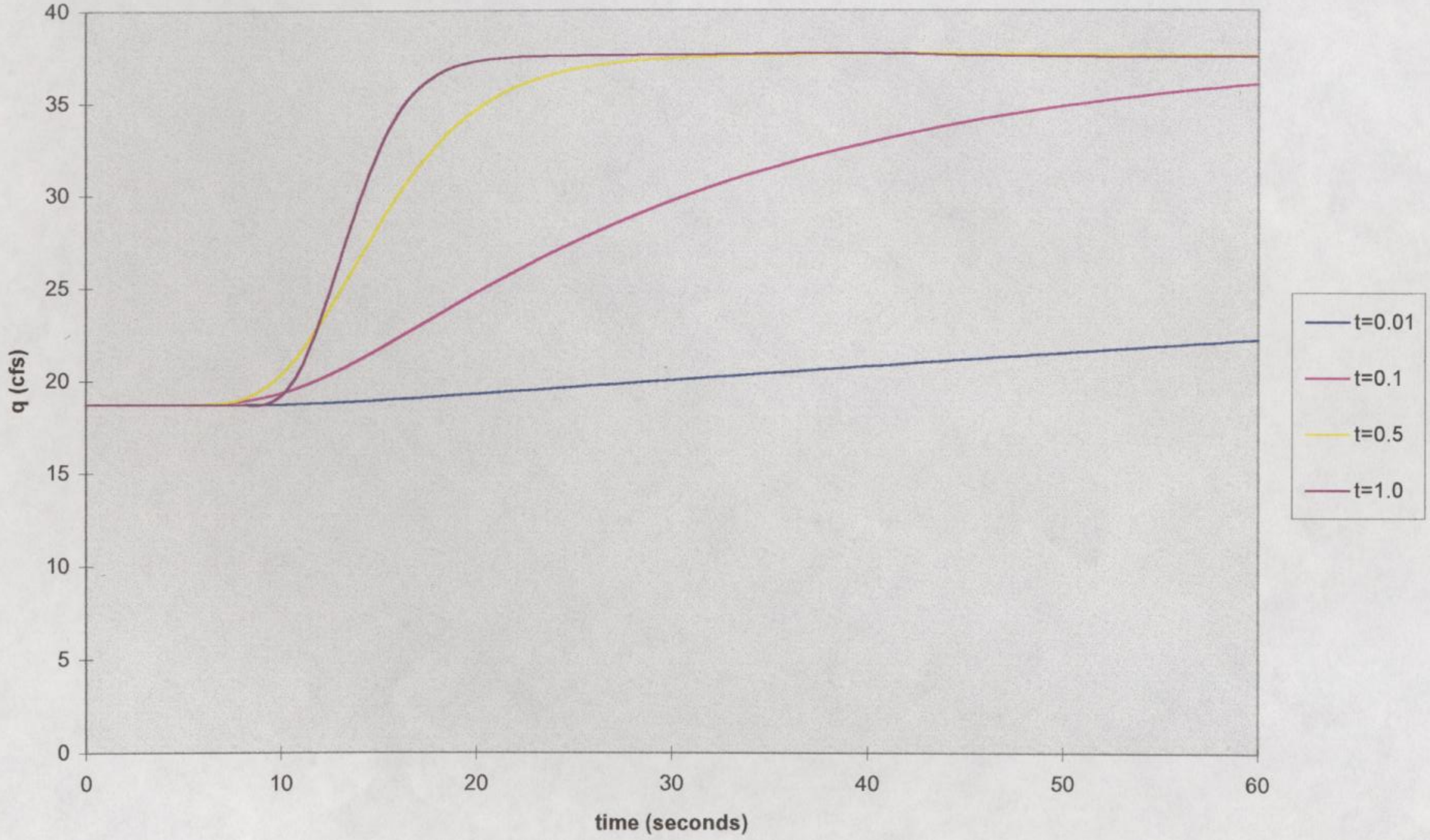

Figure 18

Saint Venant

Sensitivity to Delta t

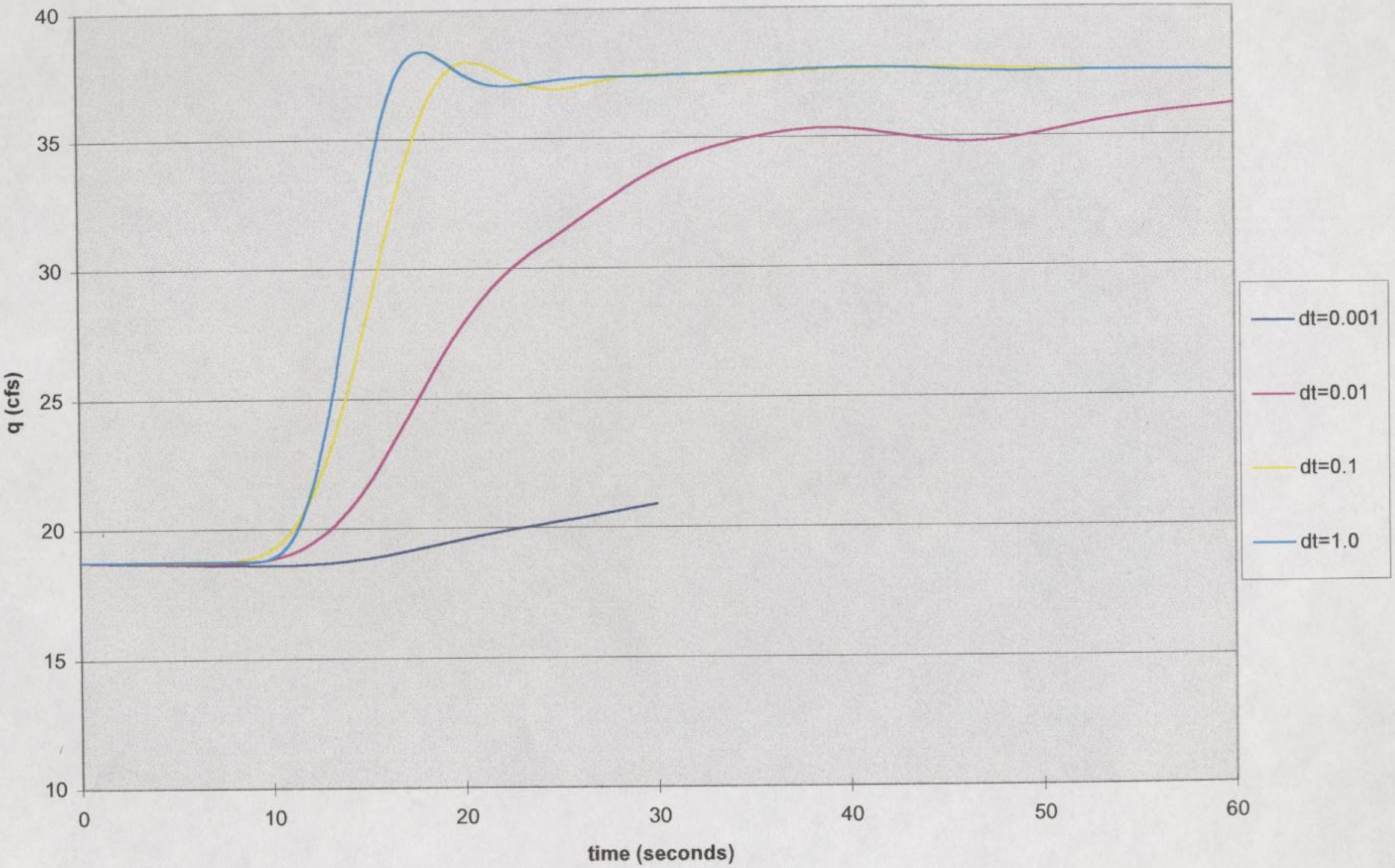

Figure 19

Method of Characteristics

Sensitivity to Delta t
Courant Number 0.994

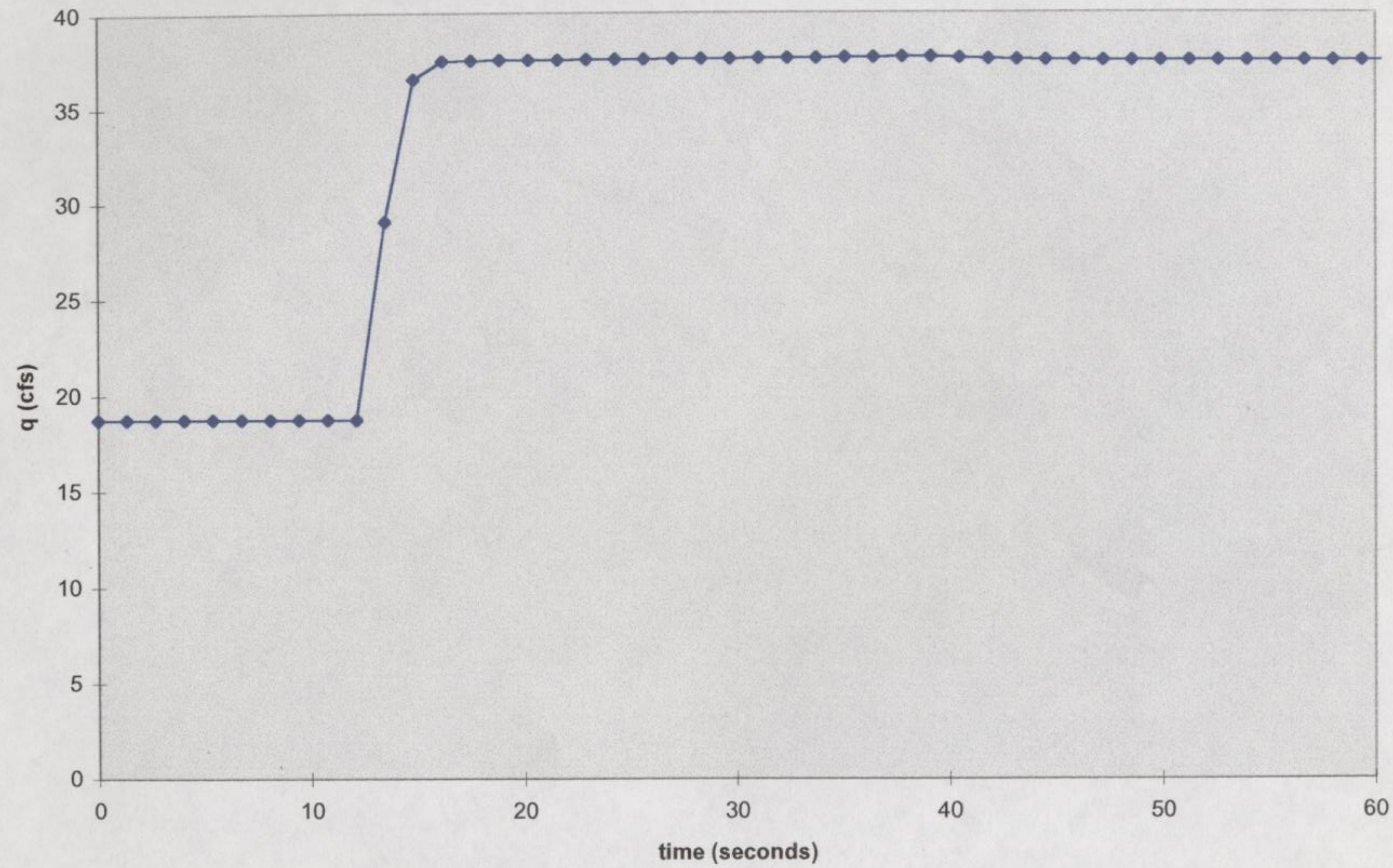

Figure 20
Saint Venant Equation

Sensitivity to Delta t
Courant Number 0.994

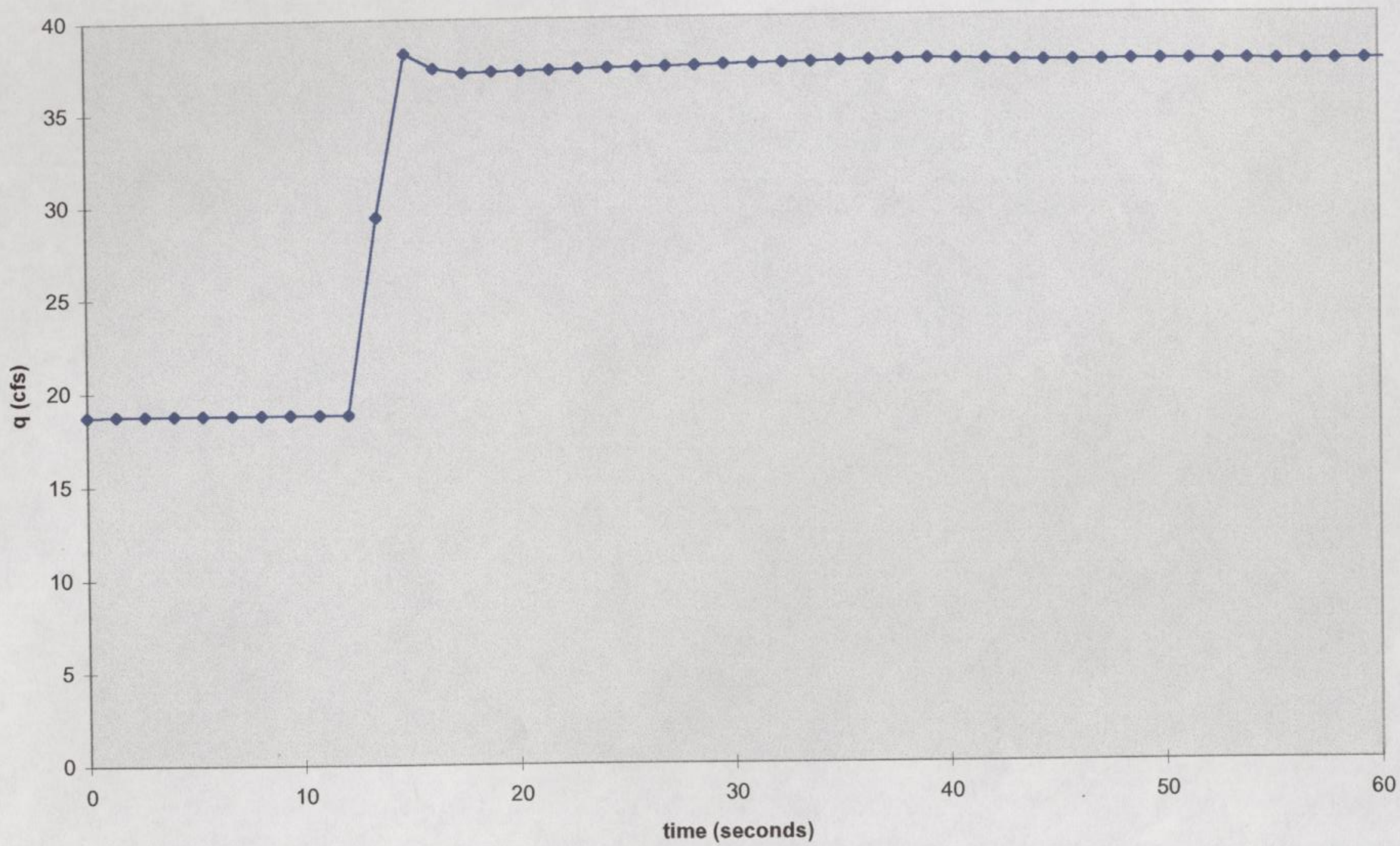

Figure 21

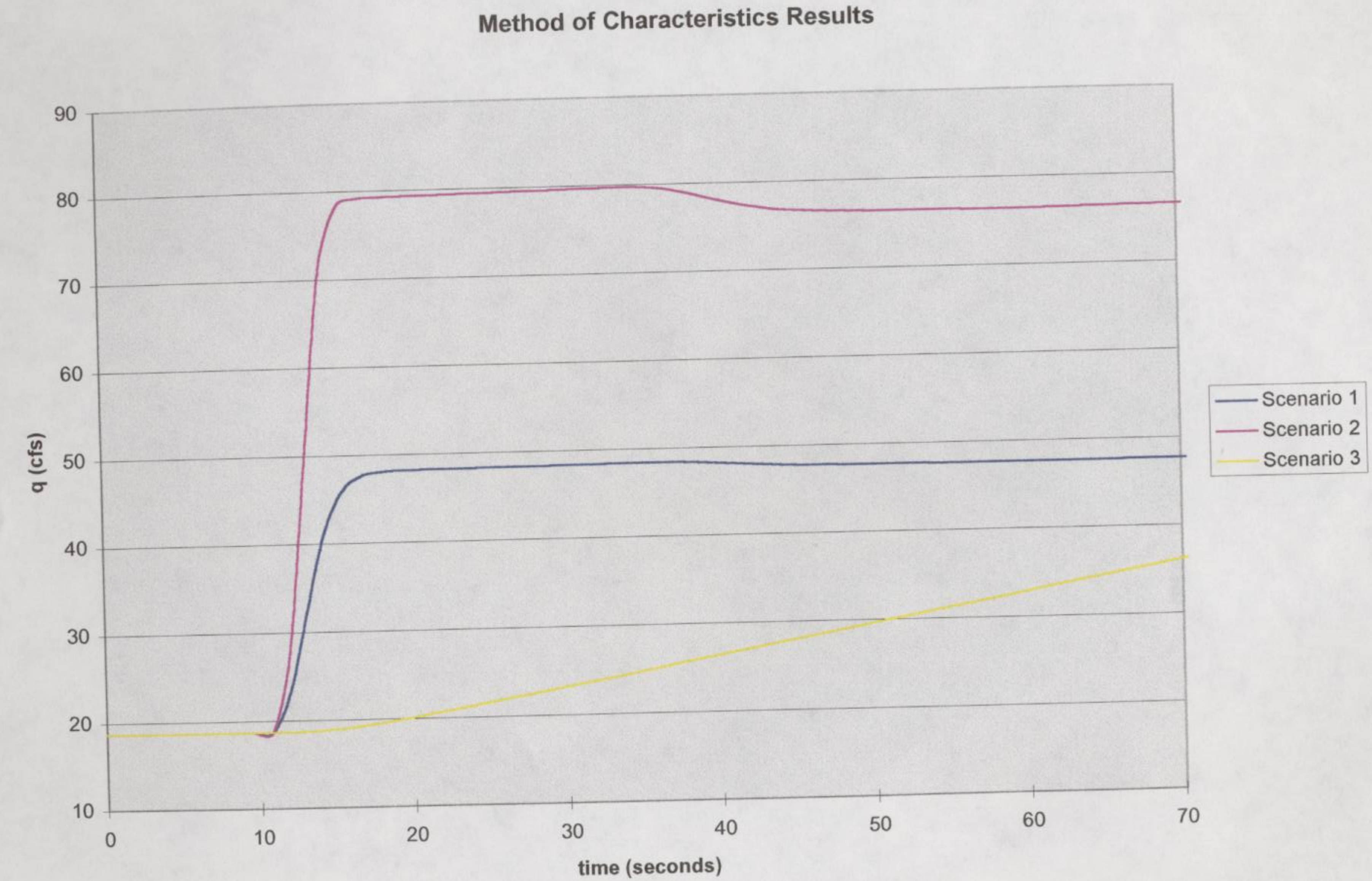

Method of Characteristics Results
q (cfs)
90
80
70
60
50
40
30
20
10
0
10
20
30
40
50
60
70
time (seconds)
Scenario 1
Scenario 2
Scenario 3

Figure 22

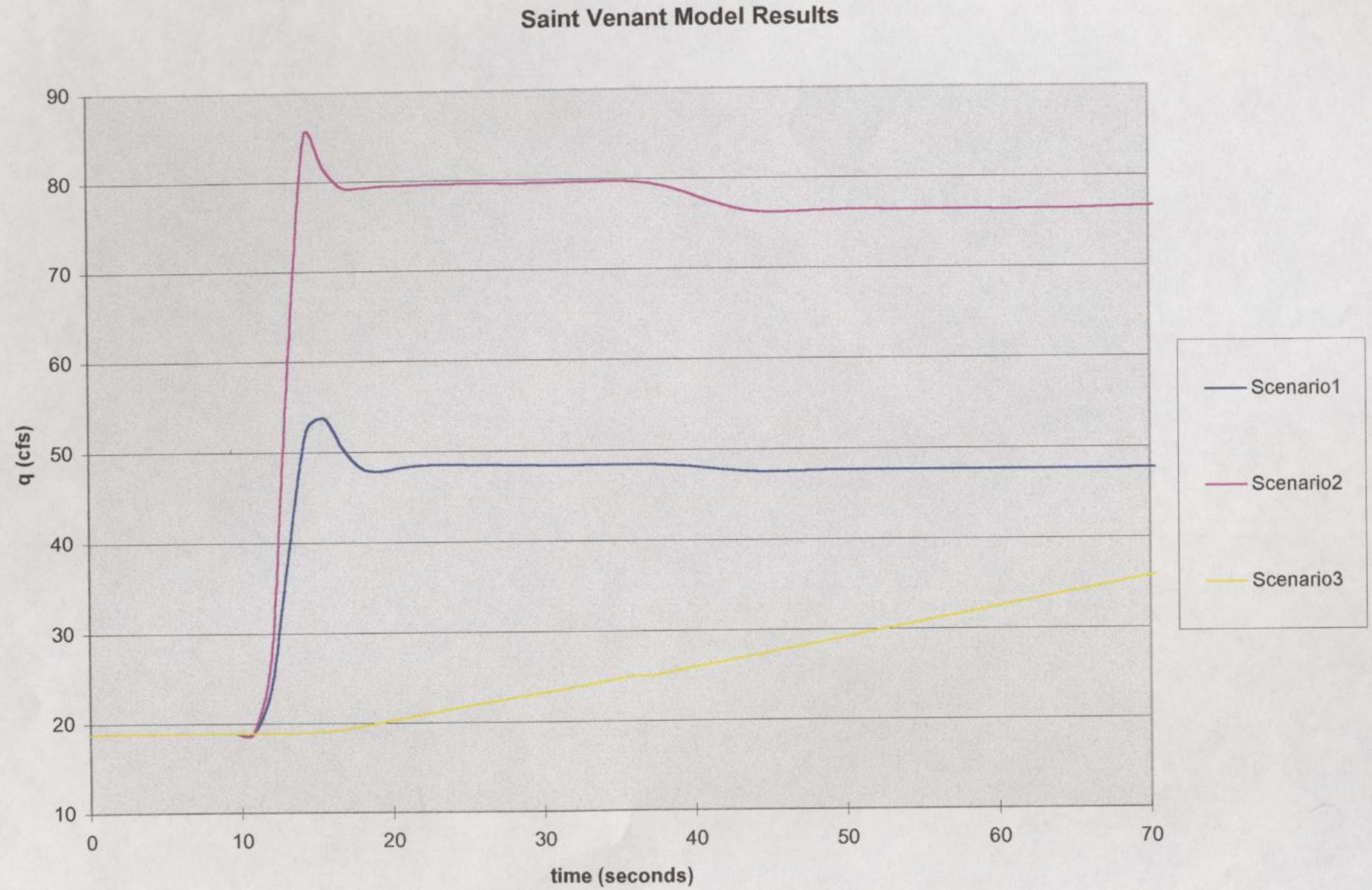
Saint Venant Model Results
q (cfs)
90
80
70
60
50
40
30
20
10
0
10
20
30
40
50
60
70
time (seconds)
Scenario1
Scenario2
Scenario3

Figure 23

Method of Characteristic: Scenario 3

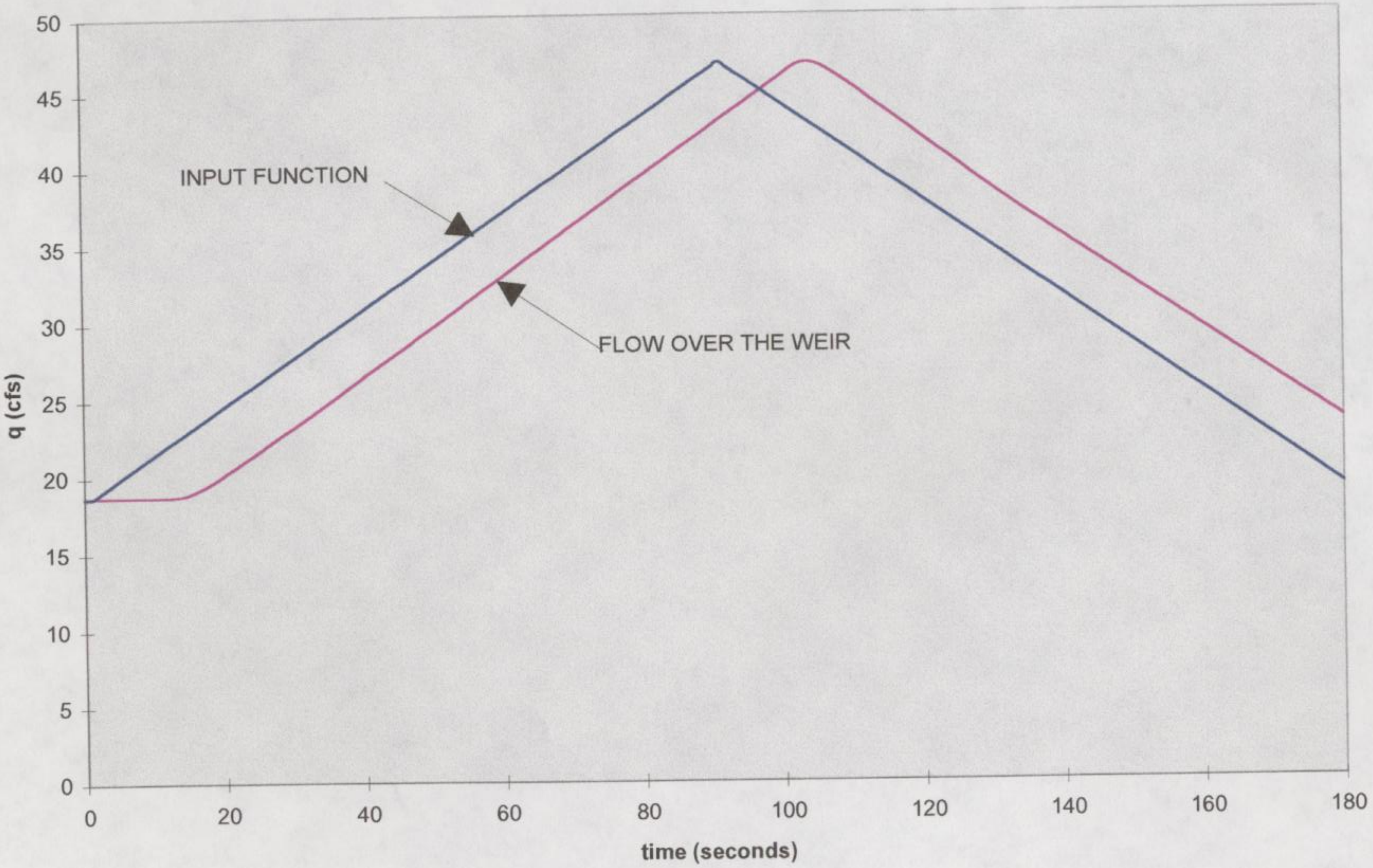

Figure 24

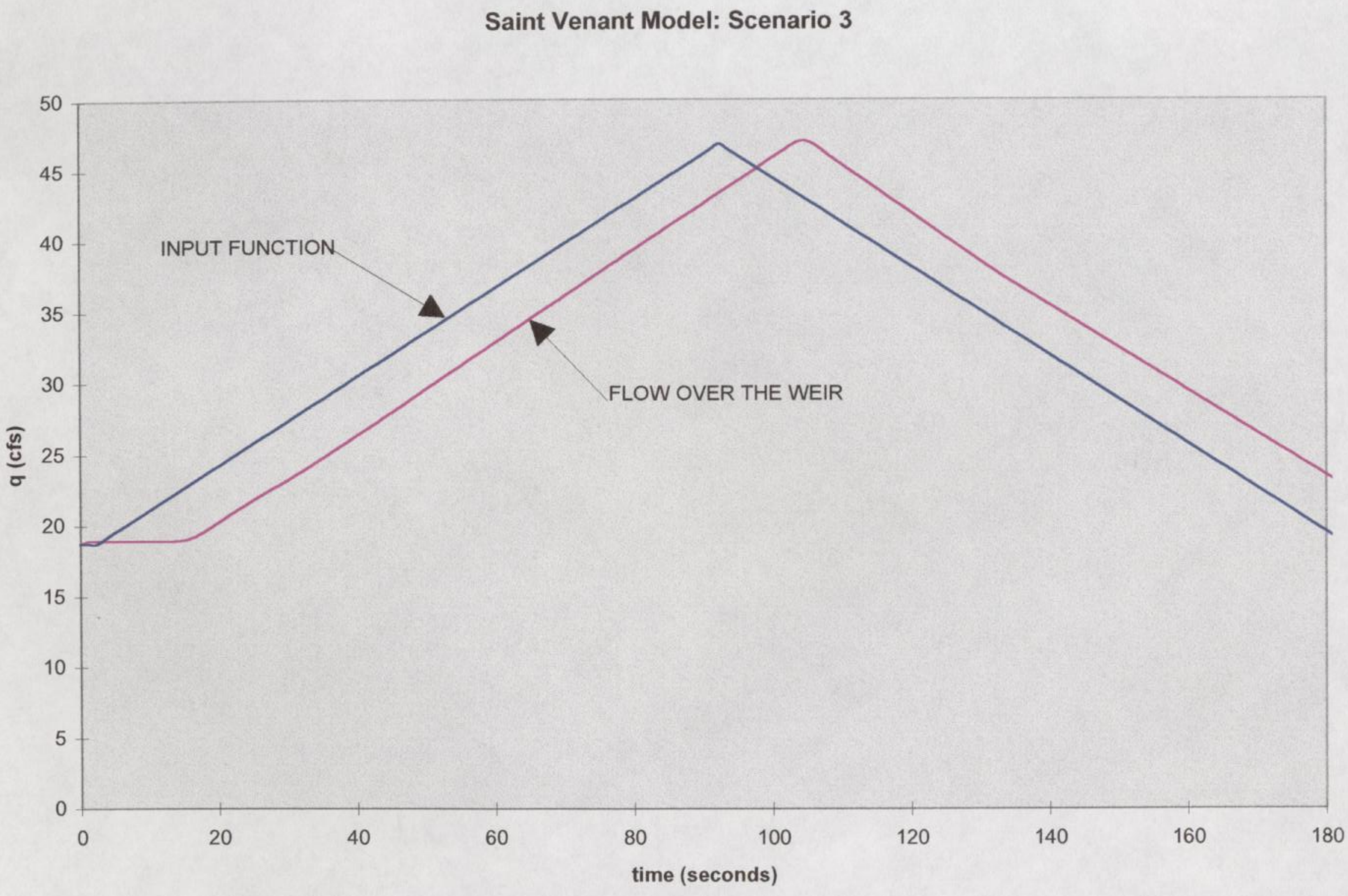

Saint Venant Model: Scenario 3
q (cfs)
50
45
40
35
30
25
20
15
10
5
0
INPUT FUNCTION
FLOW OVER THE WEIR
0
20
40
60
80
100
120
140
160
180
time (seconds)

APPENDIX A

NAME	DESCRIPTION
69DUMP.XLW	69th Street Wastewater Treatment Plant Data
VERFIC.XLS	Data used to generate Figure 10 and 11
MOCRUN5.XLS	Method of Characteristic Model with output for Figure 12
MDRUN2.XLS	Saint Venant Model with output for Figure 13
MOCRUN6.XLS	Method of Characteristic Model with output for Figure
MDRUN3.XLS	Saint Venant Model with output for Figure 15
MOCRUN7.XLS	Method of Characteristic Model with output for Figure 16
MOCRUN8.XLS	Method of Characteristic Model & output for Figures 17 & 19
MDRUN4.XLS	Saint Venant Model with output for Figure 18 and 20
MOCRUN9.XLS	Method of Characteristic Model with output for Figures 21 & 23
MDRUN5.XLS	Saint Venant Model with output for Figure 22 and 24

APPENDIX B

NAME	DESCRIPTION
REPORT.DOC	"Dynamic Modeling of the Preliminary Treatment Works at the 69th Street Wastewater Facility - Houston, Texas". 17pp
FIGURE.DOC	List of Figures, List of Tables, List of Appendix, Appendix A and B
CONTENT.DOC	Table of Contents
ACKNOW.DOC	Acknowledgments
COVER.DOC	Cover and Signature Sheets
REF.DOC	Referances